Institutionen för vattenbyggnad
Chalmers Tekniska Högskola

Department of Hydraulics
Chalmers University of Technology

Energy take-out from a wave energy device

A theoretical study of the hydrodynamics of a two-body problem consisting of a buoy and a submerged plate

by

Larry Berggren

Report Series A:23
ISSN 0348—1050 Göteborg 1992

Address: Department of Hydraulics
Chalmers University of Technology
412 96 Göteborg, Sweden

Telephone: 31–772 10 00

SUMMARY

A method for calculating the energy take-out from a single wave energy converter is presented. The converter consists of a buoy connected via a hose pump to a submerged plate. The equations of motion of the buoy and plate are solved linearly in the frequency domain, which shows that frequency dependent hydrodynamic properties can be used.

The hose pump is treated as a complex spring, the real part corresponding to a spring and the imaginary part corresponding to a time independent damping factor. The damping factor multiplied by the amplitude of the hose pump is a measure of the work done by the pump.

The drag force is linearized by setting the energy dissipation for a period equal in both the non-linear and the linear cases.

The emphasis in this report is placed on the calculation of the frequency dependent hydrodynamic properties, such as the wave excited forces and the hydrodynamic coefficients. The structure is considered to be large in comparison with the wave length and, therefore, the diffraction theory has been used. A method of calculating the forces that act on the bodies is presented, as well as the interaction between the bodies. This two-body problem is solved analytically. The present solution is compared with a numerical one and an analytical one, the latter, however, treats simply a single buoy riding in the waves.

The calculated energy take-out of the present model is compared with a time domain dependent model, and reasonable agreement has been found.

PREFACE

Research on wave/structure interaction has been carried out at the Department of Hydraulics, Chalmers University of Technology, since the mid 1970s. Wave energy devices, offshore structures and harbour units have been included.

This thesis is the result of a project to study the energy take-out of a wave energy device and this has been sponsored by the National Energy Administration, Sweden. The work has been carried out at the Department of Hydraulics and is submitted in partial fulfillment of the requirements for the degree of Technical Licentiate.

I am indebted to my colleagues at the Department of Hydraulics for their valuable contributions and for creating a stimulating work environment. I wish to thank my tutors, Professor Lars Bergdahl and Dr. Mickey Johansson, for their guidance and support. I also wish to thank Jan Forsberg (M.Sc.) and Bengt-Olof Sjöström (M.Sc., Tech. Lic.) for their contributions to the part of the work that concerned the hose-pump. I also wish to thank Ms. Yvonne Young for helping with the typing of the manuscript.

Göteborg, March 1992

Larry Berggren

CONTENTS

LIST OF TABLES

LIST OF FIGURES

LIST OF SYMBOLS

A^{ik} = added mass of body i, as a result of the motion of body k

A = the matrix containing the coefficients a_i, see Eq. 3.17

A_i = the cross sectional area of body i, perpendicular to the relative motion of body i

A_h = the non-dimensionalized amplitude of the hose pump

a_i = coefficients in the equations of motion, defined in Eqs. 3.15a - 3.15j

a^{ik} = the non-dimensionalized added mass of body i, as a result of the motion of body k

a_h = the amplitude of the hose pump

B = the wave excited forces

B^{ik} = potential damping on body i, as a result of the motion of body k

b^{ik} = the non-dimensionalized potential damping on body i, as a result of the motion of body k

C = the wave celerity

C_{D_i} = drag coefficient

C_{di} = the linearized drag coefficient of body i

C_g = the buoyancy of the buoy = $\rho\pi R^2 g$

C_g = the group celerity

d_1 = the draught of the buoy

d_2 = the thickness of the pate

E = the dissipated energy

E_{hose} = the modulus of elasticity

$E_{lin,i}$ = the dissipated energy using linearized drag coefficient

$E_{non\text{-}lin,i}$ = the dissipated energy using the non-linearized drag coefficient

E_w = the energy in the incident wave per square unit

e_{hose} = the non-dimensionalized stretching of the hose pump

e_1 = the distance from the top surface of the plate to the free surface of the fluid

e_2 = the distance from the bottom surface of the plate to the free surface of the fluid

F_{d,lin_i} = the linearized drag force on body i

F_{d_i} = the non-linearized drag force

F_i	= the forces on body i, due to the incident waves
${}_dF_i$	= the wave excited force of body i
g	= acceleration of gravity
H	= wave height
h_1	= the distance from the sea floor to the surface
h_2	= the shortest distance between body 1 and body 2
h_3	= the shortest distance from body 2 to the sea floor
j	$= \sqrt{-1}$
k	= wave number
k_{12}	= the spring stiffness of the hose pump
k_2	= the spring stiffness of the mooring system
L_{hose}	= the hose length
m_i	= the mass of body i
N	= the number of truncation terms
n	$= C_g / C$
P_w	= the power of the incident wave
p	= system pressure
R	= the radius of body i
s	= the distance travelled during one period
t	= time
v	= the relative velocity for the body
W	= the work done by the hose pump
Z	= the vector of motion, Eq. 3.18
z_i	= the motion of body i
$\hat{z}_i$	= the amplitude of body i
γ	= the imaginary part of the complex spring stiffness
η	= the efficiency of the hose pump, defined as the ratio between the work done by the hose pump and the power of the incident wave.
η_i	= the motion of the water at body i
$\hat{\eta}_i$	= the amplitude of the water at body i
λ	= the wave length
ρ	= the density of the fluid
φ_{hose}	= hose-diameter
φ_i	= the phase angles between the body i and the incident waves
ω	= the angular frequency

1. INTRODUCTION

One of the first attempts to use wave-power as a source of energy was documented in 1895, in the form of a patent for a self-propelled boat (See Fig. 1.1).

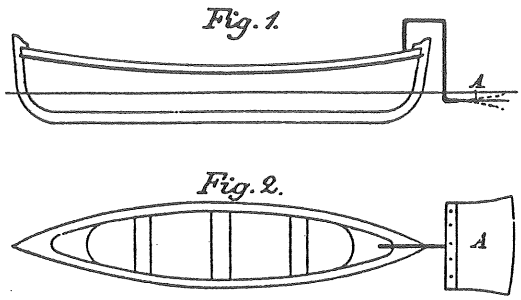

Figure 1.1 Outline drawing of a self-propelled boat, the Autonaut.

The boat was equipped with a fin located at the the stern. Due to the heave motion of the boat, the fin will bend up- and downwards propelling the boat forward. The boat could reach a velocity of 4 knots when moving against the waves. (The Naval Architect, 1979)

Since then a large number of patents has been granted for different ways of using wave power as a source of energy, but almost none of these patents have become of commercial interest. However, research in the field of wave energy increased after the oil crisis in 1973. The most active countries were Japan, Great Britain and Norway. It was also during this time that Götaverken developed the hose-pump concept, and in the beginning of the 1980s the concept was tested at Vinga, on the Swedish West Coast. A hose pump module is composed of a buoy, riding on the waves, connected to a submerged plate by an elastomeric hose. The submerged plate is, in its turn, flexibly moored to the sea floor in order to keep the module on station.

According to Hagerman (Hagerman, 1988), the function of the module is described as follows. During the passage of a wave crest, the buoy heaves up stretching the hose. The helical pattern of steel reinforcing wires in the hose causes it to constrict as it is stretched, thereby reducing its internal volume. This forces sea water out of the hose pump, through a check valve, and into a collecting hose to a turbine. After the wave crest has passed, the buoy drops down into the succeeding trough and the hose pump returns to its original length, restoring its diameter to its unstretched value. This increase in internal volume draws water into the hose through another check valve which opens to the sea. (See Fig. 1.2)

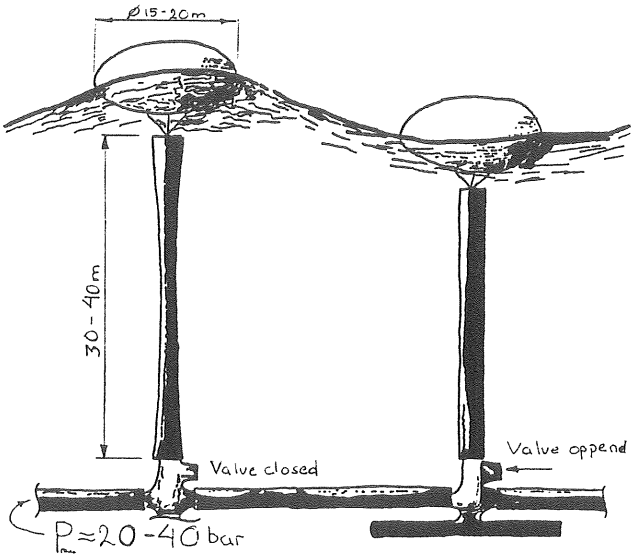

Figure 1.2 Sketch of two wave energy modules.

The test plant at Vinga consisted of three wave-energy modules that were connected to a turbine with a generator. The buoys had a diameter of 5 m, and the length of the hoses was around 10 m. From the hose pump the water was pumped into a connecting hose to a pelton turbine on shore. A hose-pump demonstration plant would consist of a considerable number of wave-energy modules, connecting hoses and a submerged turbine with a generator (See Fig. 1.3).

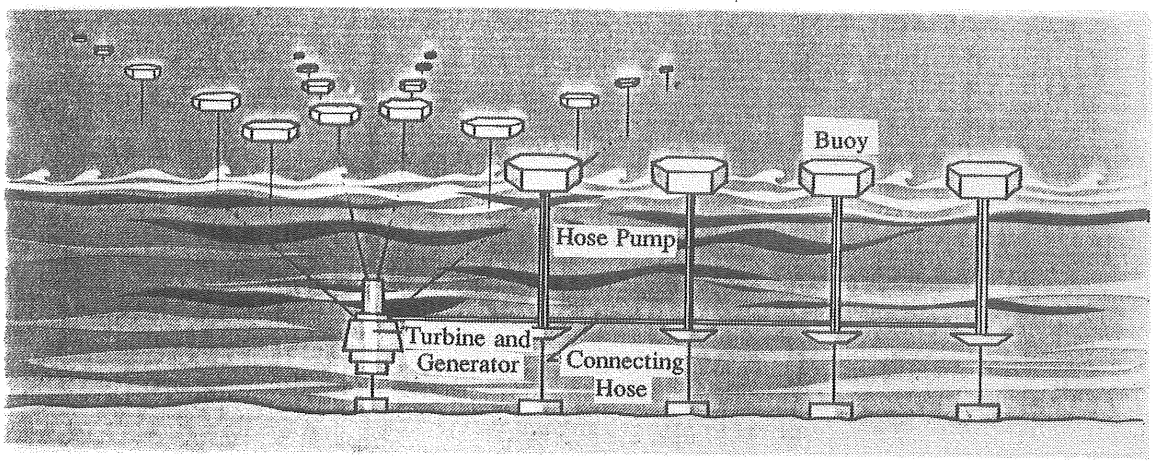

Figure 1.3 Artist's impression of the hose-pump concept

The wave-energy modules would extract some of the wave-energy from the incident waves by pumping water from these modules via the connecting hoses to the submerged turbine. The layout of the wave-energy modules depends on the direction of the incident waves. If, for instance, the main direction of the incident waves varies during the year, the modules can be arranged in a star-shaped pattern around the turbine for the most efficient energy take-out (See Fig. 1.4).

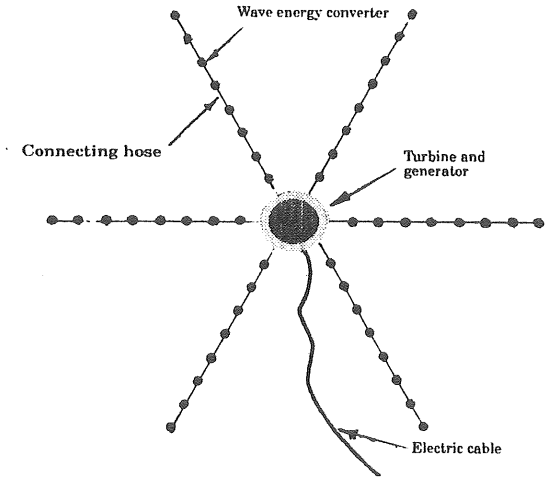

Figure 1.4 The wave energy modules arranged in a star shaped pattern around the turbine.

2 THE SCOPE OF THE WORK

The present work treats the mechanics of a single wave-energy module. The aim is to find a way to calculate the energy take-out from a single wave-energy module for different sea states. The major part of the work concerns the hydrodynamics of the buoy and the submerged plate. When calculating the forces of the incident waves that act on the buoy and submerged plate, the potential theory is used. The drag forces are not included. The problems are solved in the frequency-domain for a first order system. The calculations of the forces are described in detail in Appendices A and B. Appendix B is a conference article that describes a way to calculate the wave excited forces on the buoy and plate. Some minor corrections to the original presentation, in Japan 1991, have been made in the present article . Appendix A is an article which will be published soon in Applied Ocean Research. The article deals with the hydrodynamic coefficients of the buoy and plate.

The present work is divided into the following six major sections:

1. Formulation of the equations of motion for the buoy and the submerged plate;

2. Calculation of the characteristics of the hose-pump;

3 Calculation of the drag forces on the buoy and the submerged plate;

4 Calculation of the hydrodynamic coefficients such as added mass and potential damping;

5 Calculation of the wave-excited forces due to the incident waves; and

6. Solution of the equations of motion. This will give the amplitude and the phase angles of the buoy and the submerged plate so that the energy take-out by the module can be calculated.

3 THE EQUATIONS OF MOTION

The mathematical model consists of a buoy, a submerged plate, a hose-pump and a mooring system. The hose-pump is modelled as a complex spring and and the mooring cable as a real linear spring. Only the vertical motions are modelled. With nomenclature according to Fig. 3.1, the equations of motion of the buoy and the submerged plate can be written:

$$\begin{cases} m_1\ddot{z}_1 + k_{12}(1 + j\gamma)(z_1-z_2) + C_{d1}(\dot{z}_1 - \dot{\eta}_1) + C_g z_1 = F_1 & (3.1) \\ m_2\ddot{z}_2 + k_{12}(1 + j\gamma)(z_2-z_1) + C_{d2}(\dot{z}_2 - \dot{\eta}_2) + k_2 z_2 = F_2 & (3.2) \end{cases}$$

with:

m_i = the mass of body i
z_i = the motion of body i
k_{12} = the spring stiffness of the hose pump
γ = the imaginary part of the complex spring stiffness
C_{di} = the linearized drag coefficient of body i
η_i = the motion of the water at body i
C_g = the buoyancy of the buoy = $\rho\pi R^2 g$
k_2 = the spring stiffness of the mooring system
F_i = the forces on body i, due to the incident waves
$j = \sqrt{-1}$
Index: 1 = buoy
2 = plate

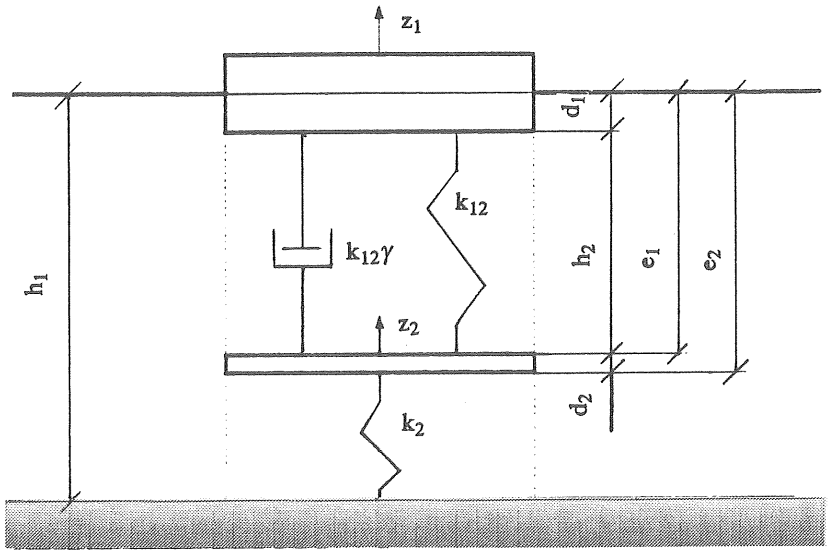

Figure 3.1 Model of a single energy converter

The incident waves are assumed to be of the form $\eta = \hat{\eta}\cos\omega t$, however complex notation is used, i.e. the motion, velocity and acceleration are the real parts of the complex expressions. The motion, velocity and acceleration for the incident wave can then be expressed as :

$$\eta_i = \hat{\eta}_i e^{j\omega t} \tag{3.3}$$
$$\dot{\eta}_i = j\omega\hat{\eta}_i e^{j\omega t} \tag{3.4}$$
$$\ddot{\eta}_i = -\omega^2\hat{\eta}_i e^{j\omega t} \tag{3.5}$$

for the buoy at the surface, i = 1 and

$$\hat{\eta}_1 = H / 2 = \text{wave amplitude;} \tag{3.6}$$

at the level of the submerged plate, i = 2 and

$$\hat{\eta}_2 = \frac{H \sinh(k(h_1 + (e_1 + e_2)/2))}{2 \sinh(kh_1)} \tag{3.7}$$

where k is the wave number, $\hat{\eta}_i$ the amplitude of the water particle at body i, and ω the angular frequency.

In a similar way one finds for the buoy and plate:

$$z_i = \hat{z}_i e^{j(\omega t + \varphi_i)} \tag{3.8}$$

$$\dot{z}_i = j\omega\hat{z}_i e^{j(\omega t + \varphi_i)} \tag{3.9}$$

$$\ddot{z}_i = -\omega^2\hat{z}_i e^{j(\omega t + \varphi_i)} \tag{3.10}$$

where $\hat{z}_i$ denotes the amplitude of body i and φ_i the phase angles between the body in question and the incident waves.

The forces on the buoy and plate due to the incident waves (omitting the drag forces) can be expressed as :

$$F_i = {}_dF_i - {}_rF_i \tag{3.11}$$

where

${}_dF_i$ = wave excited force on the body i = ${}_df_i\eta_i$

and

${}_rF_i$ = reaction forces, which are expressed as a set of hydrodynamic coefficients that are multiplied by the acceleration and the velocity of the buoy and plate.

A way to calculate the net force, F_i, that acts on the body i is as follows:

1) Keep the buoy and plate in fixed positions and let the bodies be exposed to incident waves. The wave excited forces can then be calculated by solving the diffraction problem. The way that this is carried out is described in detail in Appendix A.

2) The incident waves set the buoy and plate in motion, and the two bodies start to radiate waves in the fluid domain, which causes reaction forces on both bodies. These reaction forces are calculated in two steps by solving the radiation problem. When solving the radiation

problem there are no incident waves and the buoy and the plate, one at the time, are given a forced harmonic motion in the heave direction. The reaction forces are expressed in terms of hydrodynamic coefficients such as added mass and potential damping. The added mass indicates the part of the reaction force proportional to the acceleration of the body, and the potential damping indicates the part of the reaction force proportional to the velocity of the body.

$$ {}_rF_i = A^{ii}\ddot{z}_i + B^{ii}\dot{z}_i + A^{ik}\ddot{z}_k + B^{ik}\dot{z}_k \qquad (3.12) $$

with

A^{ik} = added mass on body i as a result of the motion of body k, and
B^{ik} = potential damping on body i as a result of the motion of body k

The calculation of added mass and potential damping is described in Appendix A.

When Eqs. 3.3 to 3.10 are substituted into Eqs. 3.1 and 3.2, one gets after division with $e^{j\omega t}$:

$$ \begin{cases} (a_1 + ja_2)\hat{z}_1 e^{j\varphi_1} + (a_3 + ja_4)\hat{z}_2 e^{j\varphi_2} = a_5\hat{\eta}_1 & (3.13) \\ (a_8 + ja_9)\hat{z}_1 e^{j\varphi_1} + (a_6 + ja_7)\hat{z}_2 e^{j\varphi_2} = a_{10}\hat{\eta}_2 & (3.14) \end{cases} $$

where :

$$ a_1 = -(m_1 + A^{11})\omega^2 + C_g + k_{12} \qquad (3.15\ a) $$
$$ a_2 = (B^{11} + C_{d1})\omega + k_{12}\gamma \qquad (3.15\ b) $$
$$ a_3 = -(A^{12}\omega^2 + k_{12}) \qquad (3.15\ c) $$
$$ a_4 = B^{12}\omega - k_{12}\gamma \qquad (3.15\ d) $$
$$ a_5 = {}_df_1 + jC_{d1} \qquad (3.15\ e) $$
$$ a_6 = -(m_2 + A^{22})\omega^2 + k_{12} + k_2 \qquad (3.15\ f) $$
$$ a_7 = (B^{22} + C_{d2})\omega + k_{12}\gamma \qquad (3.15\ g) $$
$$ a_8 = -(A^{21}\omega^2 + k_{12}) \qquad (3.15\ h) $$

$$a_9 = B_{12}\omega - k_{12}\gamma \tag{3.15 i}$$

$$a_{10} = {}_dF_2 + jC_{d2}\omega \tag{3.15 j}$$

Finally, the equation system can be rewritten in the form:

$$AZ = B \tag{3.16}$$

with

$$A = \begin{bmatrix} (a_1 + ja_2) & (a_3 + ja_4) \\ (a_8 + ja_9) & (a_6 + ja_7) \end{bmatrix} \tag{3.17}$$

$$Z = \begin{bmatrix} Z_1 \\ Z_2 \end{bmatrix} = \begin{bmatrix} \hat{z}_1 e^{j\varphi_1} \\ \hat{z}_2 e^{j\varphi_2} \end{bmatrix} \tag{3.18}$$

$$B = \begin{bmatrix} a_5 \\ \dfrac{a_{10}\sinh(k(h_1 - (e_1 + e_2)/2))}{\sinh(kh_1)} \end{bmatrix} \tag{3.19}$$

and the complex amplitudes Z_i can be calculated.

Nothing has been said so far about the linearized drag forces and the complex spring stiffness. In order to calculate the values of these variables, the amplitude and phase angle for the buoy, as well as the plate have to be known. Accordingly, in the first iteration one has to guess the amplitudes and phase angles, and then calculate the linearized drag coefficient (See Section 4) and the complex spring stiffness (See Section 5). The amplitudes and the phase angles can thereafter be calculated. If the differences between the calculated and guessed values of the amplitude and phase angles differ too much, new iterations have to be performed until the differences are acceptable.

4. THE DRAG FORCES

The drag forces on the plate and buoy are linearized as already noted, and are given as:

$$F_{d,lin_i} = C_{di}(\dot{z}_i - \dot{\eta}_i) \tag{4.1}$$

According to Morison et al., however, the drag forces are non-linear and can be expressed as:

$$F_{d_i} = C_{D_i}\rho A_i |\dot{z}_i - \dot{\eta}_i|(\dot{z}_i - \dot{\eta}_i) / 2 \tag{4.2}$$

with:

C_{D_i} = drag coefficient

ρ = the density of the ambient fluid

A_i = the cross sectional area of body i perpendicular to the relative motion of body i.

If the linearized and the non-linearized forces shall be equal, this would require that:

$$C_{D_i}\rho A_i |\dot{z}_i - \dot{\eta}_i| = C_{di} \tag{4.3}$$

which is impossible if C_{di} is to be constant.

Instead, the value of C_{di} is often adjusted so that the same amount of energy is dissipated as would be dissipated due to the non-linear drag force for one wave period. The energy that is dissipated can be calculated as:

$$\left.\begin{aligned} E &= \int_{s_o}^{s+s_o} F\,ds \\ ds &= v\,dt \end{aligned}\right\} \Rightarrow \quad E = \int_{t_o}^{T+t_o} F v\,dt \tag{4.4}$$

with:

T = the wave period
s = the distance travelled during one period length
v = the relative velocity for the body

The calculations are done for the linearized as well as the non-linearized forces, and the results are set to be equal, i.e.:

$$E_{lin,i} = E_{non\text{-}lin,i} \tag{4.5}$$

When Eqs. 4.1 to 4.4 are substituted into Eq 4.5 one gets:

$$\int_{t_o}^{T+t_o} \tfrac{1}{2}\rho C_{D_i} A_i |\dot{z}_i - \dot{\eta}_i|(\dot{z}_i - \dot{\eta}_i)^2 dt = \int_{t_o}^{T+t_o} C_{d_i}(\dot{z}_i - \dot{\eta}_i)^2 dt$$

and C_{d_i} can be expressed as:

$$C_{d_i} = \tfrac{1}{2} C_{D_i} A_i \rho \frac{\int_{t_0}^{T+t_0} |\dot{z}_i - \dot{\eta}_i|(\dot{z}_i - \dot{\eta}_i)^2 dt}{\int_{t_0}^{T+t_0} (\dot{z}_i - \dot{\eta}_i)^2 dt} \tag{4.6}$$

When solving Eq. 4.6 a problem arises, due to which the absolute value of the relative motion must be rewritten. A way to overcome this is to apply Simpson's rule to solve the upper integral in Eq. 4.6:

$$\int_{t_o}^{T+t_o} \frac{1}{2}\rho C_{D_i} A_i |\dot{z}_i - \dot{\eta}_i| (\dot{z}_i - \dot{\eta}_i)^2 dt =$$

$$\frac{1}{6} h \rho C_{D_i} A_i \left[f(x_0) + 4f(x_1) + 2f(x_2) + \ldots + 2f(x_{2n-2}) + 4f8x_{2n-1}) + f(x_{2n}) \right] + R_T \quad (4.7)$$

with:

$$h = \frac{T}{2n} \quad (4.9)$$

$$x_k = t_0 + \frac{k}{2n}(T + t_0) \quad (4.10)$$

$$f(x_k) = -j\omega^3 \left| \hat{z}_i e^{j(\omega z_k + \varphi_i)} - \hat{\eta}_i e^{j(\omega z_k)} \right| \left[\hat{z}_i e^{j(\omega z_k + \varphi_i)} - \hat{\eta}_i e^{j(\omega z_k)} \right] 2 \quad (4.11)$$

$$R_T = \frac{Th^4}{180} f^{(4)}(\xi),\ t_0 < \xi < T + t_0 \quad (4.12)$$

5 THE HOSE PUMP

The hose pump was originally intended for use in the developing countries, as a simple hand pump for pumping water from deep drilled wells. Then Götaverken (Hagerman, 1988) proposed that the hose pump also be used for extracting energy from the sea.

The hose-pump consists of a rubber hose which is reinforced with a helical shaped wire (See Figure 5.1). A critical parameter of the hose pump characteristics is the slope angle of the wires. When the hose is stretched and the cross sectional area of the hose decreases, the internal volume of the hose will also decrease if, and only if, the slope angle exceeds a certain value. For smaller values of the slope angle, the volume will remain constant during the pump cycle.

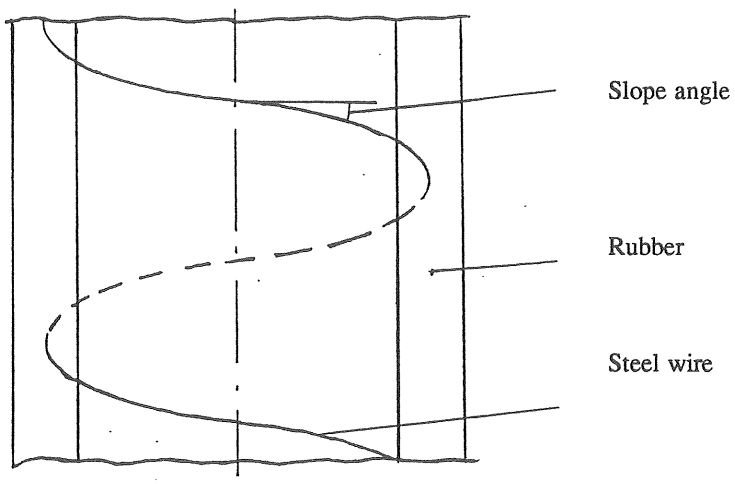

Figure 5.1 Outline diagram of the hose

A mathematical model of the hose-pump, for calculating the energy take-out, was developed by Technocean in the beginning of the 1980s (Forsberg, 1991). As the

model is non-linear, the equations are described in the time domain and, therefore, cannot be used here. However, from this time-model Technocean has derived a new, simplified, linear model which describes the characteristics of the hose pump in the frequency domain (Technocean, 1991). The new model is calibrated to the old model which in turn is calibrated according to the results of the field test that was performed at Vinga.

In the new model, approximations are made for the most important pump characteristics. All algorithms are continuous within a limited stretching range which allows a Maclaurin expansion of the first order for the most important pump characteristics such as the pressure force and the elastic force. The Maclaurin expansion is developed around the average value of the non-dimensionalized stretching, $1 + e_o$. In the frequency model, the physical behaviour of the pump is taken into consideration and two conditions are stated concerning the pressure:

1) When the pressure present in the pump exceeds the system pressure, water is pumped into the connecting hose.

2) When the pressure present is below the system pressure, water is pumped into the pump from the surrounding fluid.

It is beyond the scope of this work to derive the formulae of the pump characteristics from the time domain to the frequency domain and, therefore, the model will be treated as a "black box". Input data to the black box are the hose length (L_{hose}), hose-diameter (φ_{hose}), the modulus of elasticity (E_{hose}), system pressure (p_{hose}) and the strain (e_{hose}) and the relative motion of the hose pump. The output from the model is the complex spring stiffness, $k_{12}(1 + j\gamma)$. The real part, k_{12}, corresponds to the real spring stiffness, and the imaginary part, $k_{12}\gamma$, corresponds to a velocity independent damping constant from which the energy take-out can be calculated.

6 COMPARISON BETWEEN THE PRESENT SOLUTION AND A SOLUTION BASED ON THE INTEGRAL EQUATION METHOD

In Appendices A and B a comparison is made, between the present solution and a solution for a single floating cylinder (Johansson, 1986), of the wave excited forces and the hydrodynamic coefficients. In the case of the single cylinder the same method of matched eigenfunction expansion was used. In order to avoid influencing the results, the plate was kept close to the sea-floor. The wave excited force and the hydrodynamic coefficients for the plate have not, so far, been compared with the results from any other program. In this section, therefore, a comparison is made between the present solution and a numerical one (Lei & Bergdahl, 1992). The numerical solution is based on the integral equation method, also known as the panel method.

When calculating the wave excited force, the following geometrical properties were chosen (See Fig. 3.1):

R / h_1	$= 0.2$	$h_2 / h_1 = 0.3$
d_1 / h_1	$= 0.1$	$h_3 / h_1 = 0.5$
d_2 / h_1	$= 0.1$	

The wave excited forces on the plate and the buoy are non-dimensionalized by dividing by the factor $\pi\rho g H R^2 / 2$. From Fig 6.1, it can be seen that for frequencies approaching zero, the dimensionalized force that acts on the buoy approaches the lift force of a cylinder of radius R and draught H / 2, i.e. the wave excited force is equal to $\pi\rho g H R^2 / 2$, and then, for increasing frequencies, the wave excited force decreases to zero. The wave excited force on the plate approaches zero for frequencies approaching zero. Then, for increasing frequencies, the wave excited force on the plate first increases until it reaches a maximum value, a value that is less than $\pi\rho g H R^2/2$, and thereafter it decreases and approaches zero.

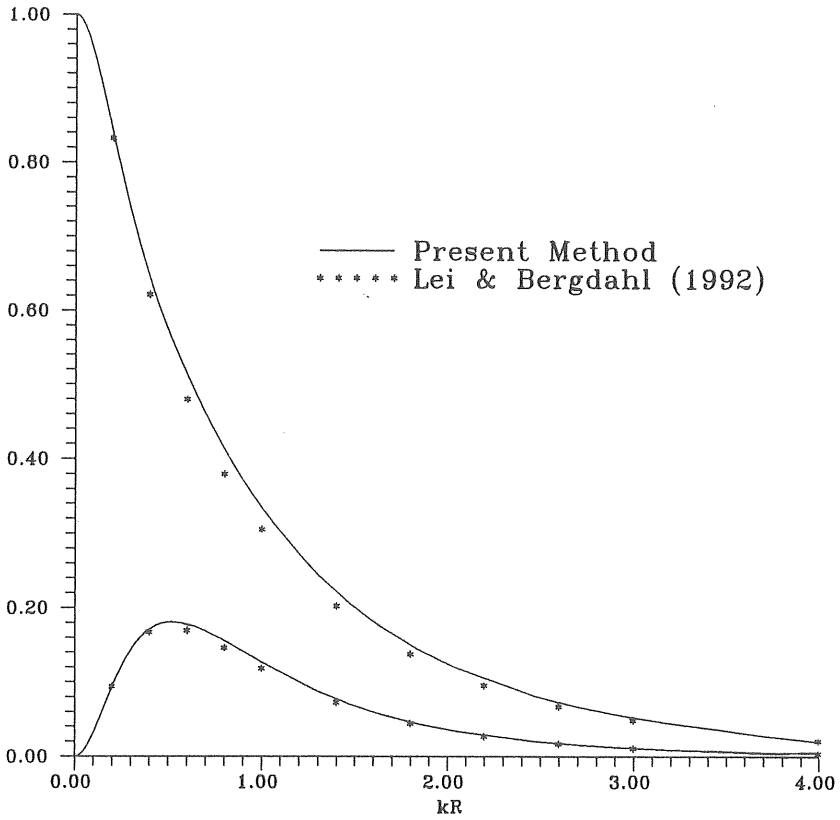

Figure 6.1 Non-dimensional wave excited forces for the buoy and plate as a function of kR, with k = the wave number and R = the radius.

When comparing the hydrodynamic coefficients, added mass and potential damping, the same geometrical properties were chosen. The added mass was non-dimensionalized by dividing by the mass of a hemisphere, $2\pi\rho R^3 / 3$ and the potential damping was also non-dimensionalized by dividing by the mass of a hemisphere multiplied by the present frequency, $2\pi\rho R^3\omega / 3$. From Figs. 6.2 and 6.3, it can be seen that the damping of the buoy is greater than that of the plate, i.e. the buoy radiates more energy to the fluid domain than the plate. From the figures it can also be seen that the added mass of the plate is larger than that of the buoy, due to the fact that the plate is surrounded by fluid whereas the buoy is free on one side. From Figs. 6.4 and 6.5, it can be seen that the hydrodynamic coefficients, as a result of the motion of the other body, are equal.

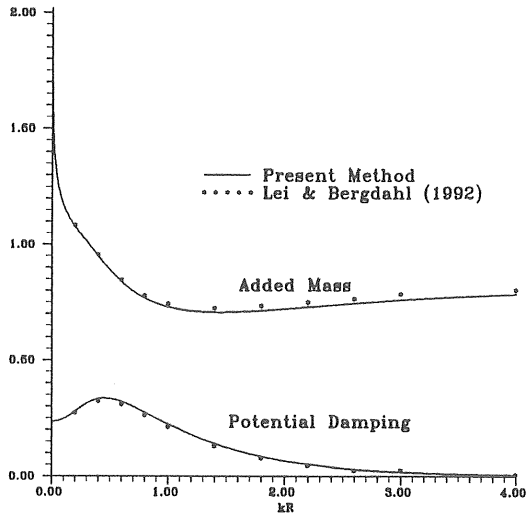

Figure 6.2 Added mass and potential damping of the buoy, as a consequence of the motion of the buoy. kR = the wave number multiplied by the radius of the buoy.

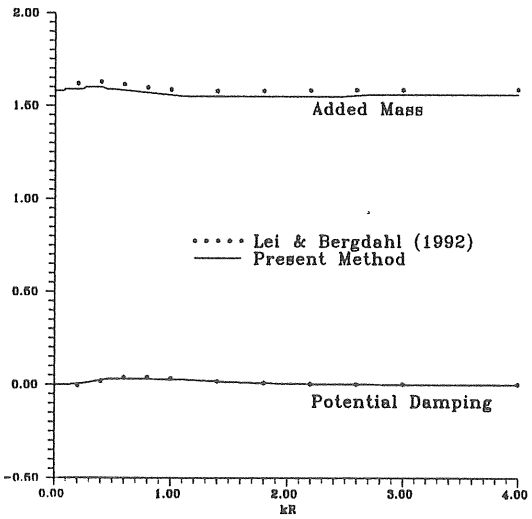

Figure 6.3 Added mass and potential damping of the plate, as a consequence of the motion of the plate. kR = the wave number multiplied by the radius of the buoy.

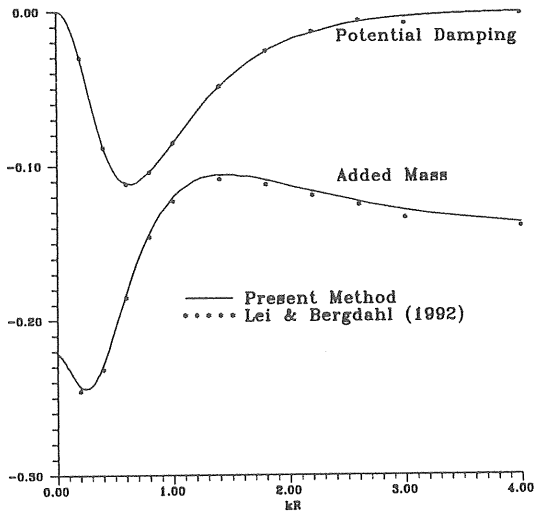

Figure 6.4 Added mass and potential damping of the plate, as a consequence of the motion of the buoy. kR = the wave number multiplied by the radius of the buoy.

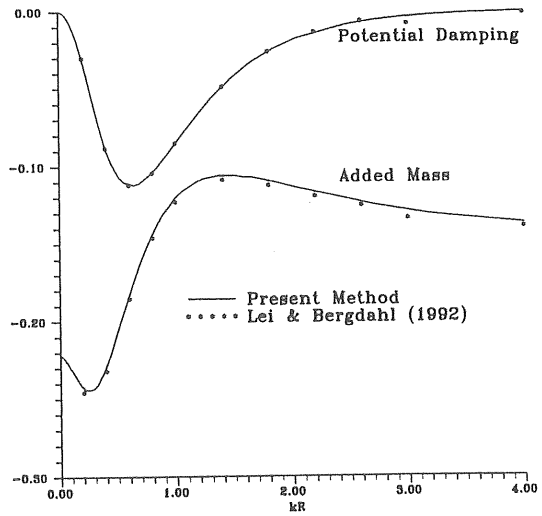

Figure 6.5 Added mass and potential damping of the buoy, as a consequence of the motion of the plate. kR = the wave number multiplied by the radius of the buoy.

The agreement between the present method and the numerical one is acceptable for both the wave excited forces and the hydrodynamic coefficients.

The present solutions of the wave excited forces and hydrodynamic coefficients are analytically derived and are obtained in the form of infinite series. Therefore, when the values are evaluated on the computer, the series have to be truncated and the accuracy of the answers depend on the number of terms, N, in the series. It is desirable to keep the number of terms as low as possible and still obtain an answer that satisfies the required accuracy. The time consuming part of the program is the solution of an equation system of the form: AX = B with A as a (3N x 3N) matrix and B a 3N vector. In Table 6.1, an example is given for the convergence for increasing N.

Table 6.1

Truncation characteristics for the wave excited forces and the hydrodynamic coefficients ($d_1/h_1 = 0.25$, $R/h_1 = 0.50$, $h_2/h_1 = 0.74$, $h_3/h_1 = 0.01$, $d_2/h_1 = 0.0$, and $kR = 0.821$)

N	a^{11}	b^{11}	a^{22}	b^{22}	F_1	F_2
5	1.16	0.291	1.16	0.518e-5	0.960	0.405e-2
10	1.17	0.291	1.22	0.528e-5	0.960	0.409e-2
20	1.18	0.291	1.27	0.571e-5	0.960	0.426e-2
30	1.18	0.291	1.28	0.583e-5	0.960	0.430e-2
40	1.18	0.291	1.29	0.591e-5	0.960	0.433e-2
50	1.18	0.291	1.30	0.595e-5	0.960	0.434e-2

7. RESULTS

In this section the amplitudes and phase angles of the buoy and the plate are calculated. This is done in two steps. First the amplitudes and phase angles are calculated, for a system without any drag forces and with the spring stiffness of the hose pump and mooring cable equal to zero. The equations of motion are then reduced to:

$$\begin{cases} m_1\ddot{z}_1 + C_g z_1 = F_1 & (7.1) \\ m_2\ddot{z}_2 + \quad\;\; = F_2 & (7.2) \end{cases}$$

In the second step the amplitudes and the phase angles of the buoy and the plate are obtained, by solving Eqs. 3.1 and 3.2. In the examples presented here, the characteristics of the buoy and the plate are not changed and the following numerical values are chosen:

R	$= 7.5$ m	h_2	$= 38.93$ m
d_1	$= 0.34$ m	h_3	$= 20.64$ m
d_2	$= 0.09$ m	m_1	$= 32.5 \cdot 10^3$ kg
h_1	$= 60$ m	m_2	$= 30.0 \cdot 10^3$ kg
$C_{D,buoy}$	$= 0.9$	$C_{D,plate}$	$= 1.9$

When the wave excited forces and the hydrodynamic coefficients are calculated, the truncation term, N, is set to 20.

The characteristics yielded for the hose pump are:

$L_{hose} = 22$m	= length of the hose
$\phi_{hose} = 0.6$ m	= the diameter of the hose pump
$p_{hose} = 1.05$MPa	= the system pressure
$e_{hose} = 0.05$	= the main strain of the hose

For the purpose of including the drag terms, the wave steepness is set to 0.03, that is, the wave height becomes:

$H = 0.03\lambda = 0.06\pi / k$

with λ = wave length and k = wave number.

In Figures 7.1 - 7.2 the wave excited forces and the hydrodynamic forces are presented, and they are non-dimensionalized by the same factors as in Section 6. From Figure 7.1 it is seen that the wave excited force on the plate is comparatively small. In figure 7.2 the hydrodynamic coefficients, $a^{(11)}$, $b^{(11)}$ and $a^{(22)}$ are shown. The potential damping of the plate, $b^{(22)}$, and the cross terms, $a^{(21)}$, $a^{(12)}$, $b^{(21)}$ and $b^{(12)}$ are very small, due to the relatively great distances between the buoy and the plate and between the plate and the bottom, and, therefore, are not presented.

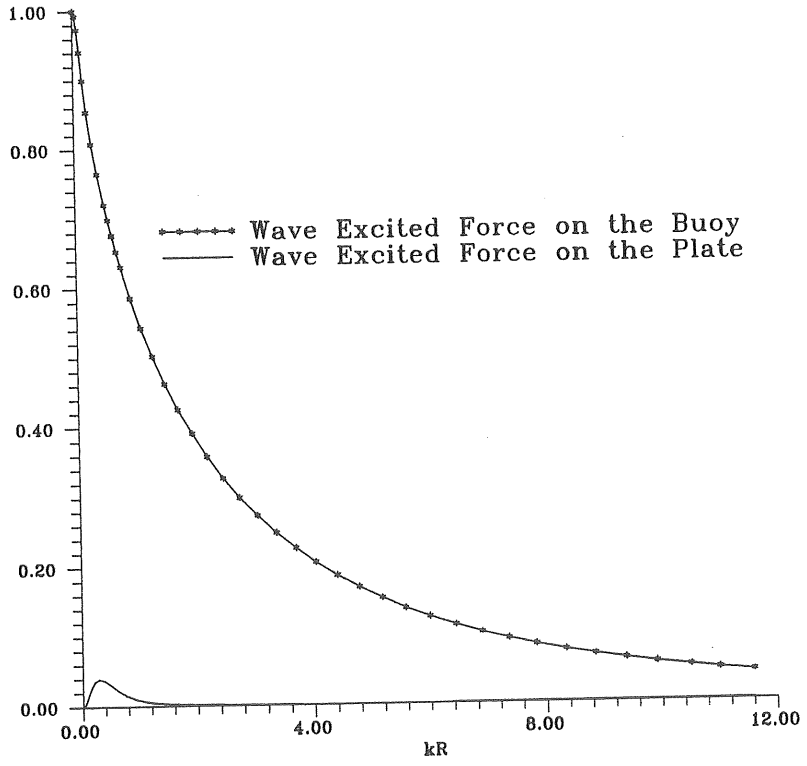

Figure 7.1 The non-dimensionalized wave excited forces on the buoy and plate.

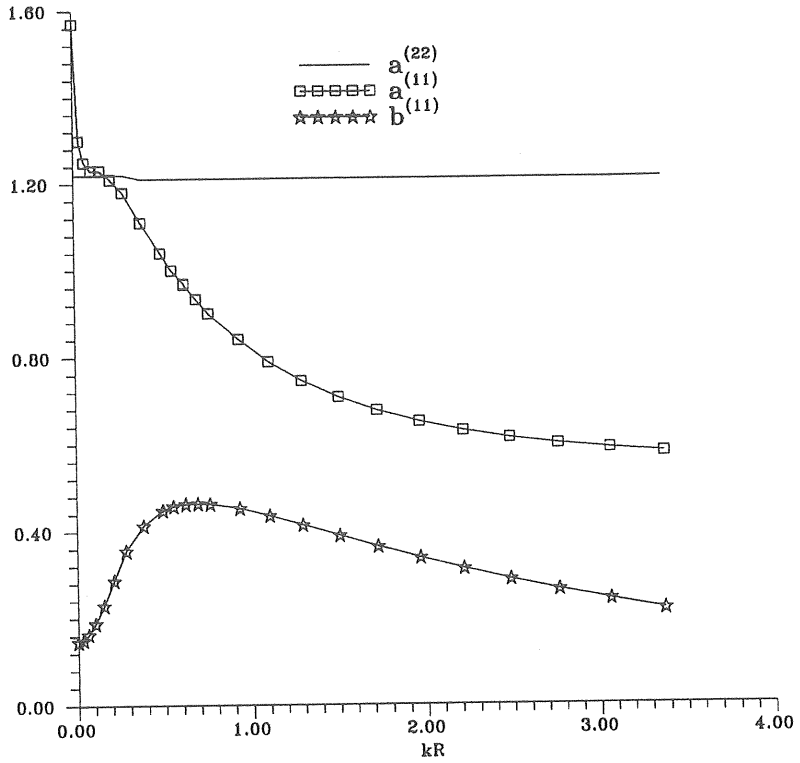

Figure 7.2 The hydrodynamic coefficients of the buoy, $a^{(11)}$ and $b^{(11)}$, and added mass of the plate $a^{(22)}$.

In Figure 7.3 the amplitudes of the buoy and the plate are presented. When comparing the amplitudes of the buoy for the two cases, it can be seen that they are equal to the wave amplitude for small frequencies, i.e. $\omega \to 0$. The resonance peak is almost damped out and is moved towards a frequency lower for the second case than for the first case. The plate for the second case also has an amplitude that is equal to the wave amplitude for small frequencies. It can be shown that for small frequencies the plate will always have an amplitude equal to the wave amplitude, as long as the spring stiffness is greater than zero. It should be pointed out that the numerical model of the hose pump is a good approximation only when the relative amplitude of the hose pump is within

certain limits. The relative motion is normalized by the length of the hose:

$$A_h = \frac{\{\{\hat{z}_1 \cos(\varepsilon_1) - \hat{z}_2 \cos(\varepsilon_2)\}^2 + \{\hat{z}_2 \cos(\varepsilon_2) - \hat{z}_1 \cos(\varepsilon_1)\}^2\}^{\frac{1}{2}}}{L_{hose}} \quad (7.1)$$

To get a correct value for the spring stiffness of the hose pump, the relative motion must be less than 5% and more than 1%. For motions more than 5% or less than 1%, the spring stiffness can be given the constant values that are yielded for the 5% and 1% motions, respectively. When the relative motion is between 5% and 1%, it can be seen that the plate will have an almost constant value for amplitude. For the case without a hose pump, case one, the plate will have an amplitude equal to the amplitude at the corresponding depth.

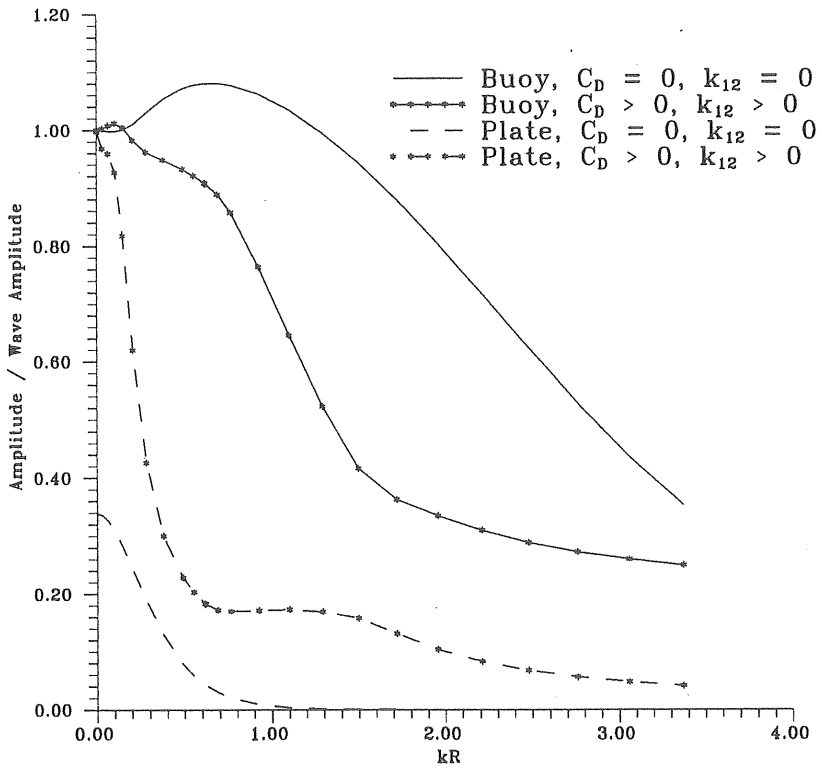

Figure 7.3 Non-dimensionalized amplitudes of the buoy and the plate.

Figure 7.4 shows that the phase angles of both the plate and the buoy are in phase with the incident waves for low frequencies. The phase angles for the buoy and the plate in the first case are almost identical, but for the second case the difference between the phase angles increases for increasing frequencies until it reaches a constant value.

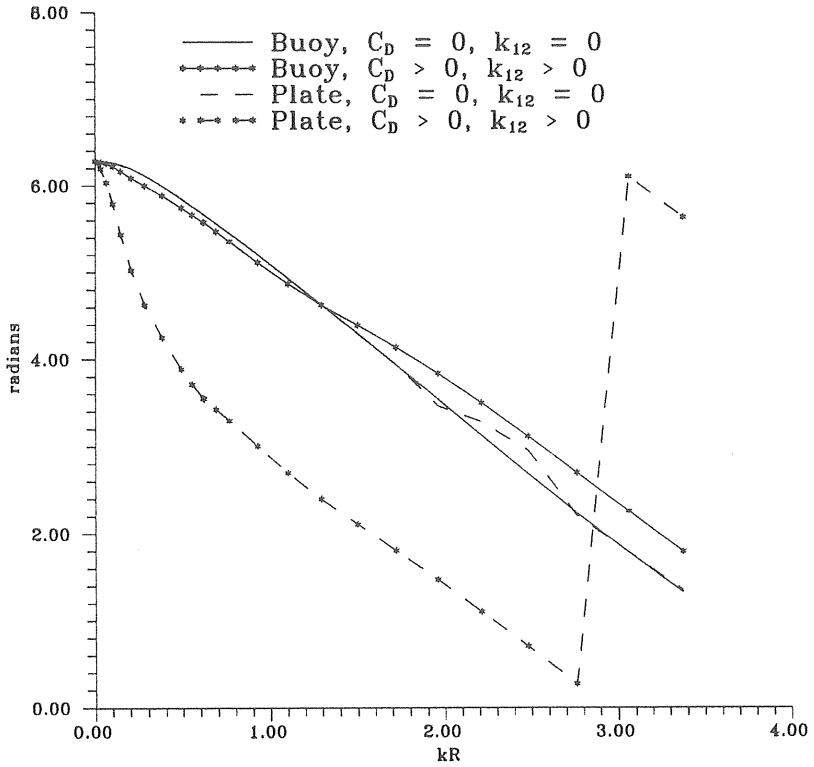

Figure 7.4 Phase angles for the buoy and the plate

Figure 7.5 shows the relative motion of the hose pump, i.e. Eq. 7.3, and also shows that the hose pump behaves as one might expect. For low frequencies the motion is zero, then it increases to a maximum, the resonance peak, followed by a decrease to zero.

When the hose pump was linearized, one of the conditions was that the work done by the hose pump should be independent of the duration of a pump cycle. The different phases of one pump cycle, building up the pressure, pumping water into the connecting hose, and refilling the hose pump, are diagrammed as a distorted rhombus (Fig. 7.5) in the time domain model, however, in the present model the pump cycle is simplified to an ellipse. The area of this ellipse corresponds to the work done by the hose pump and can be calculated as:

$$W = \pi a^2 k_{12} \tau / T \qquad (7.4)$$

where

$$a_h = A_h \cdot L_{hose}$$

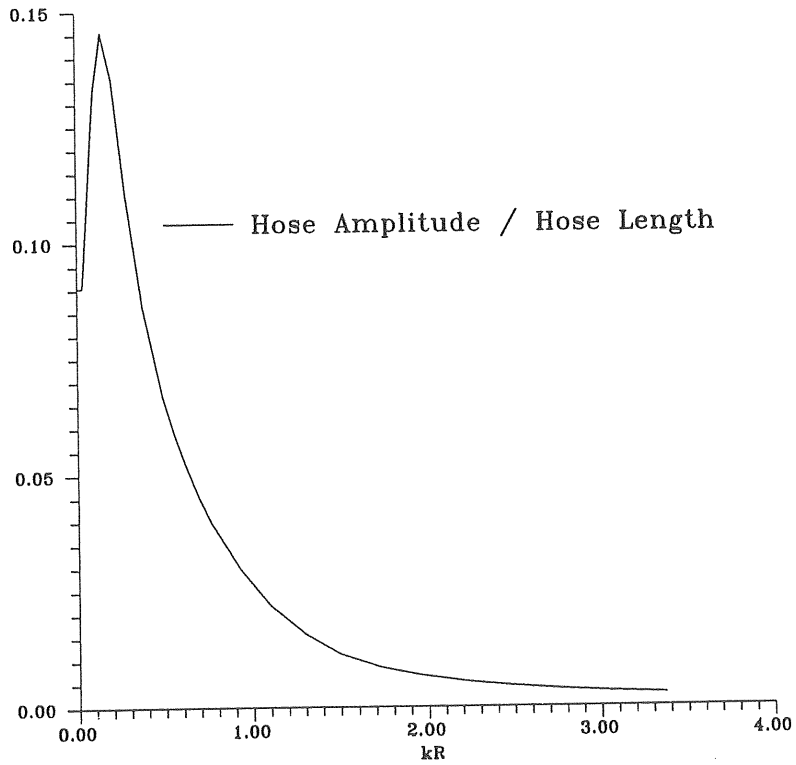

Figure 7.5 The non-dimensionalized amplitude of the hose

In the first phase, 1, the pressure is built up and all valves are closed. In the second phase, 2, the pressure continues to grow due to the elastic force in the hose and water is also pumped from the hose into the connecting hose. In the third phase, 3, the pressure decreases and the volume increases, all valves are closed. In the fourth phase, 4, the pressure is below the system pressure, a valve is opened and the pump is filled with water.

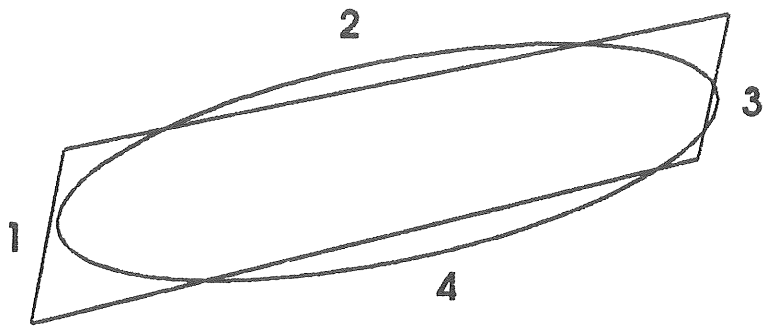

Figure 7.6 The different pump phases for the hose pump. The longer radius corresponds to the amplitude of the hose pump and the shorter radius corresponds to the imaginary part of the complex spring stiffness.

One way to calculate the efficiency (Bergdahl, 1979) is to calculate the work done by the hose pump divided by the power of the incident waves that pass through a width equal to the buoy diameter. This efficiency number is called the capture-width ratio.

The power in the incident waves can be calculated by

$$P_w = E_w C_g 2R \tag{7.5}$$

with

$$E_w = \frac{\rho g H^2}{8} = \text{energy / square unit} \tag{7.6}$$

$C_g = nC$ = group celerity (7.7)

$C = \lambda / T$ = wave celerity (7.8)

$$n = \tfrac{1}{2}\{ 1 + \frac{4\pi h_1}{\lambda \sinh(4\pi h_1 / \lambda)} \} \quad (7.9)$$

λ = wave length.

Substituting Eqs. (7.6) to (7.9) into Eq. (7.5) yields

$$P_w = \frac{\rho g H^2 \lambda R}{8T} \cdot \{ 1 + \frac{4\pi h_1}{\lambda \sinh(4\pi h_1 / \lambda)} \} \quad (7.10)$$

and finally, the capture-width ratio can be calculated as

$$\eta = \frac{8\pi (A_h L_{hose})^2 k_{12} \tau}{\rho g H^2 R} \cdot \{ \frac{\sinh(4\pi h_1 / \lambda)}{4\pi h_1 + \lambda \sinh(4\pi h_1 / \lambda)} \} \quad (7.11)$$

Figure 7.7 shows the capture-width ratio as a function of kR. One can see two maxima, of which the first corresponds to the case when the relative motion of the hose is over 5% and the spring stiffness is given a constant value. When the relative motion is below 5% the spring stiffness will alter for each frequency, and one can see that this will increase the capture-width ratio. The capture-width ratio then grows to a second peak value which is close to 40%, after which it decreases to zero.

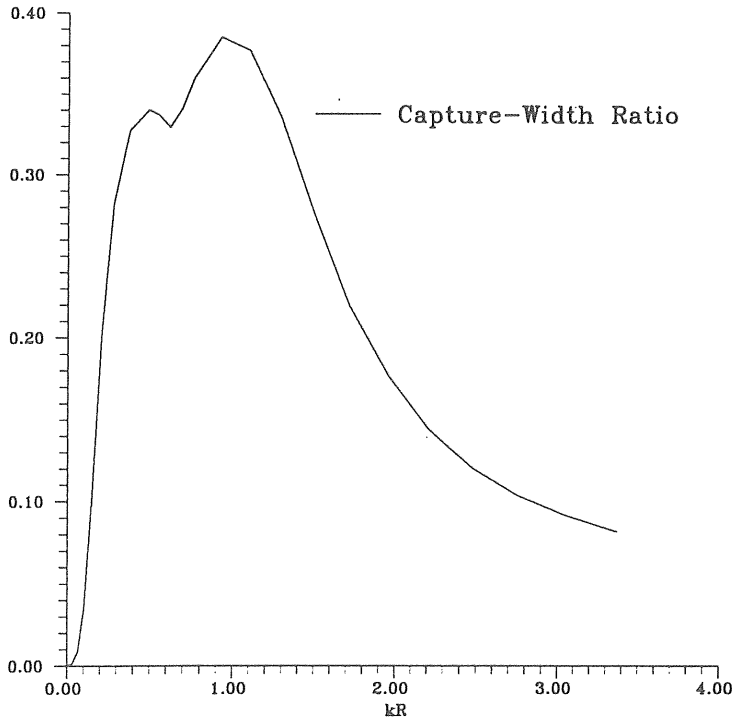

Figure 7.8 Capture-width ratio as function of the non-dimensionalized wave number.

Finally, a comparison is shown between the present model and the time domain model that was developed by Technocean. While the time domain model describes the hose pump more accurately, the present model, on the other hand, describes the hydrodynamic coefficients and the wave excited forces more accurately. The geometric properties are identical to the input data presented in the beginning of this section. The comparison is made for two cases.

Input Data:	$m_1 = 30 \cdot 10^3$ kg		= the mass of the buoy
	$m_2 = 35 \cdot 10^3$ kg		= the mass of the plate
	Case 1	H = 2.28 m	= wave height
		ω = 1.047 rad/s	= the angular frequence
	Case 2	H = 1.52	= wave height
		ω = 1.257 rad/s	= the angular frequence

Output Data:

	Case 1		Case 2	
	T.D.M	P.M.	T.D.M	P.M
Added Mass, $a^{(11)}$	0.716	0.871	0.716	0.763
Added Mass, $a^{(12)}$	0.0	$-0.30 \cdot 10^{-2}$	0.0	$-0.23 \cdot 10^{-2}$
Added Mass, $a^{(21)}$	0.0	$-0.30 \cdot 10^{-2}$	0.0	$-0.23 \cdot 10^{-2}$
Added Mass, $a^{(22)}$	2.046	1.21	2.046	1.21
Pot. Damp., $b^{(11)}$	0.466	0.459	0.466	0.424
Pot. Damp., $b^{(12)}$	0.0	$-0.10 \cdot 10^{-1}$	0.0	$-0.49 \cdot 10^{-2}$
Pot. Damp., $b^{(21)}$	0.0	$-0.10 \cdot 10^{-1}$	0.0	$-0.49 \cdot 10^{-2}$
Pot. Damp., $b^{(22)}$	0.0	$-0.23 \cdot 10^{-3}$	0.0	$0.56 \cdot 10^{-4}$
A_h	6.2%	4.8%	3.6%	2.45%
η	19%	17%	35%	27%

with:

T.D.M = Time Domain Model and
P.M = Present Model

Although the efficiency calculated for the two models agrees, further comparisons are necessary to validate the model proposed here.

8 CONCLUSIONS

This study concerns the energy take-out from a wave energy module consisting of a buoy connected via a hose pump to a submerged plate. To calculate the energy take-out the stretching of the hose pump has to be estimated from the motions of the buoy and the plate. The equations of motion for the buoy and plate therefore have to be solved. The equations of motion are solved in the frequency domain and contain the mass of the buoy and plate (physical and added mass), damping of the buoy and plate (potential damping and damping due to drag force), the wave excited force on the buoy and plate and finally the behaviour of the hose pump.

The emphasis in this report is placed on the calculation of wave excited force (the diffraction problem), and the added mass and the potential damping (the radiation problem). Both the diffraction problem and the radiation problem are solved analytically. When solving the radiation problem the cross terms are also solved, i.e. the added mass and the potential damping on body i caused by an oscillation of body j. It is concluded that, for the tested realistic geometry, the cross terms are less than a few percent of the added mass and the potential damping on body i caused by its own motion. As mentioned above the problems are solved analytically which, when run on a computer, requires much less CPU-time than numerical solutions. The results have been tested against other solutions, one analytical solution (Johansson, 1987) and one numerical one (Lei & Bergdahl, 1992) and the agreement is satisfactory.

The energy take-out calculated from the present model agrees acceptably with that from a specially tailored time domain model. For two cases, the capture-width ratios calculated from the present model are 17% and 27% and from the time domain model 19% and 35% respectively.

A suggestion for future work is the development of an optimization method for a single energy converter in a given wave climate. In connection with this model, tests would be valuable. It would also be of interest to study the interaction between several converters in order to see if it is possible to model theoretically a complete wave energy-plant by the method of matched eigenfunctions.

References

1. Wave Energy for Propelling Craft - Nothing New. The Naval Architect, Nov. 1979.

2. Hagerman G. W., Wave Energy Resource and Technology Assessment for Coastal North Carolina. SEASUN Power System, Alexandria, Virginia, USA 1988.

3. Forsberg J., Personal consultation. Department of Hydraulics, Chalmers University of Technology, Jan. 1992.

4. Forsberg J. and Sjöström B-O., Överföring av slangpumpens kraftekvationer till frekvensplanet (In Swedish), Report number 9106, Göteborg, Sweden, Sept. 1991.

5. Johansson M., Transient Motion of Large Floating Structures. Lic. Eng. Thesis, Report A:14, Department of Hydraulics, Chalmers University of Technology, 1987.

6 Lei X. and Bergdahl L., Hydrodynamic Properties of Multiple Floating and Submerged Bodies Analyzed by a Panel Method. To be presented at the Boundary Elements and Fluid Dynamics Conference, Southampton, Great Britain, Apr. 1992.

7. Bergdahl L., Effektupptagning i oregelbundna vågor hos en vågboj med linjär dämpning (In Swedish). Gruppen för vågenergiforskning, Gr:5, Department of Hydraulics, Chalmers,Sweden, Aug. 1979.

Hydrodynamic coefficients of a wave energy device consisting of a buoy and a submerged plate.

LARRY BERGGREN and MICKEY JOHANSSON
Dept. of Hydraulics, Chalmers University of Technology,
412 96 Göteborg, Sweden.

Hydrodynamic coefficients of a wave energy device, consisting of a buoy connected to a submerged plate, are presented. Both the buoy and the plate are idealized as vertical cylinders. For this two-body system, the case with the buoy oscillating vertically and the case with the submerged plate oscillating vertically are treated. The coefficients are solved by the method of matched eigenfunction expansions. Numerical results showing the plate's influence on the hydrodynamic coefficients of the buoy and vice versa are presented.
Key Words: Wave power, radiation problem, two-body system, hydrodynamic coefficients

1. INTRODUCTION

A buoy riding in waves, connected to a submerged plate by an elastomeric hose, has been proposed as a device for extraction of energy from waves.[1] The elastomeric hose acts as a pump that is driven by the relative motion between the buoy and the submerged plate. The submerged plate is moored to the sea floor. The concepts is according to Hagerman described below.[1] During the passage of a wave crest, the buoy heaves up, stretching the hose. The helical pattern of steel reinforcing wires in the hose causes it to constrict as it is stretched, thereby reducing its internal volume. This forces sea water out of the hose pump, through a check valve, and into a collecting line to a turbine. After the wave crest has passed, the the buoy drops down into the succeeding trough and the hose pump returns to its original length, restoring its diameter to its unstretched value. This increase in internal volume draws water into the hose through another check valve, which is open to the sea. (See Fig. 1)

In order to analyze the dynamics of the wave energy device, properties such as hydrodynamic coefficients have to be calculated. The problem is formulated linearly here which means that the coefficients associated with the harmonic

motion of one of the bodies are calculated assuming the other body as fixed. The radiated waves associated with the body in motion cause dynamic pressure. In a two-body system, this pressure will not only be experienced by the body in motion but also by the fixed body. This will give an added mass and damping coefficient for the body in motion as well as cross-terms for added mass and damping of the fixed body. In this paper added mass and potential damping including cross-terms are calculated for the cases with vertical motions of each of the two bodies.

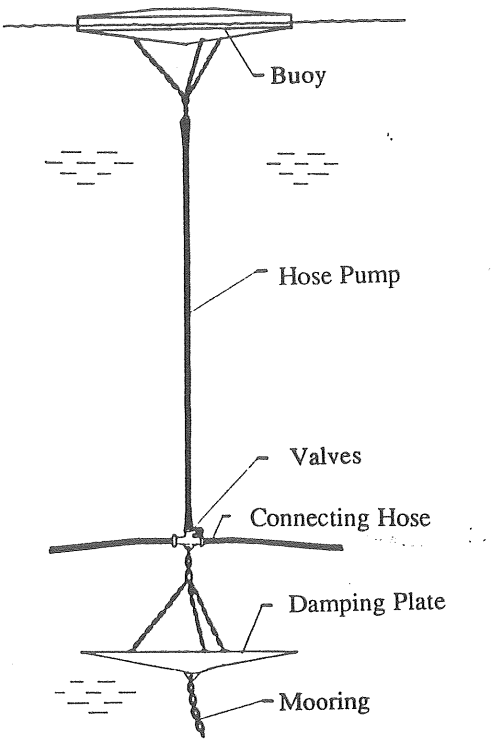

Figure 1 The hose pump concept. Elastomeric hose acts as a pump, that is driven by the relative heaving motion between buoy and submerged plate.

The nomenclature of added mass and potential damping is retained throughout the report also for the cross-terms, which should be kept in mind to avoid confusion. The added mass of both the fixed and moving bodies is then defined as a quantity that, multiplied with the acceleration of the moving body, gives part of the hydrodynamic force on the body which is in phase with the acceleration of the moving body. In a similar way, the potential damping is defined as a quantity, that, multiplied by the velocity of the moving body, gives that part of the hydrodynamic force on the body which is in phase with the velocity of the moving body. The wave energy device is idealized as two vertical cylinders of equal diameter. For such a geometry, the problem is suitably solved by the method of matched eigenfunction expansions, a technique in which the fluid domain is divided into sub domains. In each subdomain an eigenfunction expansion of the velocity potential is constructed. The technique has been used for both two-dimensional problems (see [2,3,4]) and and axisymmetric three-dimensional problems (see [5,6])

2. FORMULATION OF THE PROBLEM

The geometrical properties of the idealized wave energy device are defined in Figure 2. A cartesian coordinate system, Oxyz, as well as a cylindrical coordinate system , Orθz, is defined with the origin in the undisturbed free surface and the z-axis positive upwards. The buoy occupies the space defined as $r \leq R$, $0 \leq \theta \leq 2\pi$, $z \geq -d_1$ and the submerged plate occupies the space defined as $r \leq R$, $0 \leq \theta \leq 2\pi$, $-e_2 \leq z \leq -e_1$.

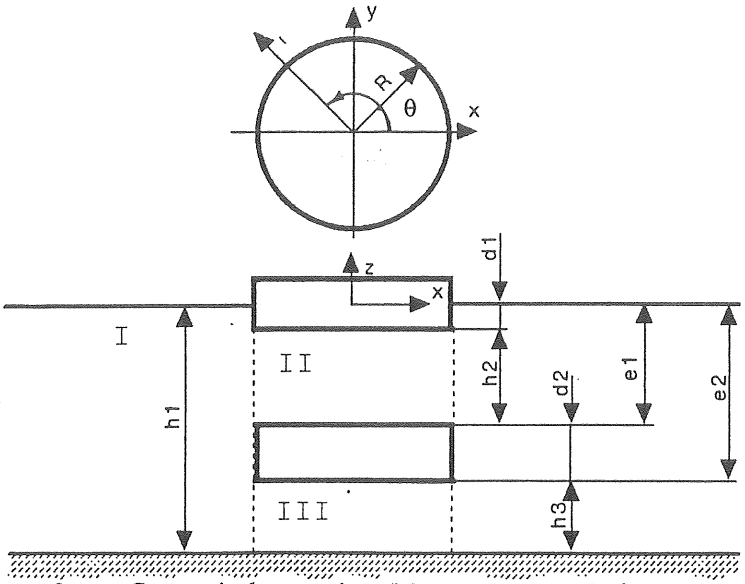

Figure 2 Geometrical properties of the wave energy device and definition of fluid sub domains.

Small oscillating vertical motions are assumed. The flow is considered irrotational and the fluid incompressible. If the amplitude of the vertical motion of the buoy is denoted ζ, then the flow is suitably described by the velocity potential $\mathrm{Re}\{-i\omega\zeta\phi(r,z)\exp(-i\omega t)\}$ ($i = \sqrt{-1}$, ω = angular frequency and t = time) where the spatial part of the velocity potential ϕ, is governed by the following boundary-value problem:

$$\frac{\partial^2\phi}{\partial z^2} + \frac{1}{r}\frac{\partial}{\partial r}\left(r\frac{\partial\phi}{\partial r}\right) = 0 \qquad (1)$$

$$\frac{\partial\phi}{\partial z} - \frac{\omega^2}{g}\phi = 0 \qquad (z = 0,\ r \geq a) \qquad (2)$$

$$\frac{\partial \phi}{\partial z} = 0 \qquad (z = -h_1) \qquad (3)$$

$$\frac{\partial \phi}{\partial z} = 1 \qquad (z = -d_1, r < R) \qquad (4)$$

$$\frac{\partial \phi}{\partial z} = 0 \qquad (z = -e_1, r < R) \qquad (5)$$

$$\frac{\partial \phi}{\partial z} = 0 \qquad (z = -e_2, r < R \qquad (6)$$

$$\frac{\partial \phi}{\partial r} = 0 \qquad (-d_1 < z < 0, r = R) \qquad (7)$$

$$\frac{\partial \phi}{\partial r} = 0 \qquad (-e_2 < z < -e_1, r = R) \qquad (8)$$

$$\lim \sqrt{r} \left(\frac{\partial \phi}{\partial r} - ik\phi \right) = 0 \text{ when } (r \to \infty) \qquad (9)$$

where k is the wave number. In the case for which the plate oscillates the boundary value problem will be changed only slightly. The changes appear in boundary conditions (4), (5) and (6). They become

$$\frac{\partial \phi}{\partial z} = 0 \qquad (z = -d_1, r < R) \qquad (10)$$

$$\frac{\partial \phi}{\partial z} = 1 \qquad (z = -e_1, r < R) \qquad (11)$$

$$\frac{\partial \phi}{\partial z} = 1 \qquad (z = -e_2, r < R) \qquad (12)$$

3. SOLUTION

In the solution procedure, the fluid domain is divided into three sub domains as indicated in Figure 2. The method of separation of variables is applied in each sub domain in order to obtain expressions for the unknown function, i.e. the velocity potential. Expressions valid in each sub domain are obtained as infinite series of orthogonal functions. These expressions are developed to satisfy all

boundary conditions except at the boundaries joining the sub domains, i.e. at r=R. It then remains to determine the unknown coefficients in the series. This is done by imposing the condition of continuity of pressure and normal velocity at r=R. Mathematically, this is fulfilled by matching the potentials and the normal derivatives of the potentials, respectively.

The formulation starts from the potentials developed independently in each sub domain.
Applying the method of separation of variables gives the spatial potentials in each region expressed in terms of orthogonal series. In region I, the potential becomes

$$\phi_1 = \sum_{n=1}^{\infty} A_n \cos\lambda_n(z+h_1) \frac{R_n(\lambda_n r)}{R_n(\lambda_n R)} \qquad (13)$$

where the eigenvalues are

$$\begin{aligned} &\lambda_1 = -ik \quad \text{where k is the wave number} \\ &k \tanh kh_1 = \omega^2/g && n=1 \\ &\lambda_n \tan \lambda_n h_1 = -\omega^2/g && n=2,3.. \end{aligned} \qquad (14)$$

and the radial function R_n is

$$\begin{aligned} &R_1(\lambda_1 r) = H_o^{(1)}(i\lambda_1 r) = H_o^{(1)}(kr) && n=1 \\ &R_n(\lambda_n r) = K(\lambda_n r) && n=2,3.. \end{aligned} \qquad (15)$$

where $H_o^{(1)}$ is the Hankel function of first kind and zeroth order and K_o is the modified Bessel function of second kind and zeroth order.

In region II, the potential and corresponding eigenvalues become:

$$\phi_2 = \phi_{2p}^{(i)} + \sum_{n=1}^{\infty} B_n \cos \beta_n(z+e_1) \frac{I_o(\beta_n r)}{I_o(\beta_n R)} \qquad (16)$$

$$\beta_n = (n-1)\pi/h_2 \tag{17}$$

where I_o is the modified Bessel function of first kind and zeroth order. The superscript (i) of the particular solution is used to identify which one of the two bodies oscillates. The superscript 1 refers to the case when the buoy oscillates and 2 refers to the case when the plate oscillates. The particular solution becomes

$$\overset{(i)}{\phi_{2p}} = \begin{cases} \dfrac{(z+e_1)^2 - r^2/2}{2h_2} & i = 1 \\ -\dfrac{(z+d_1)^2 - r^2/2}{2h_2} & i = 2 \end{cases} \tag{18}$$

In region III, the potential and corresponding eigenvalues become

$$\phi_3 = \overset{(i)}{\phi_{3p}} + \sum_{n=1}^{\infty} C_n \cos\gamma_n(z+h_1) \frac{I_o(\gamma_n r)}{I_o(\gamma_n R)} \tag{19}$$

$$\gamma_n = (n-1)\pi/h_3 \tag{20}$$

where the particular solution is given by

$$\overset{(i)}{\phi_{3p}} = \begin{cases} 0 & i = 1 \\ \dfrac{(z+h_1)^2 - r^2/2}{2h_3} & i = 2 \end{cases} \tag{21}$$

The potentials given above describe the flow in each region and satisfy all boundary conditions except those at r = R. For example, in region I the potential satisfies the linear free surface boundary condition, the impermeable bottom condition and the radiation condition when $r \to \infty$.

The remaining problem is mainly to determine the three sets of unknown coefficients $\{(A_n, B_n, C_n), n=1,2,...\}$. The three sets are found by imposing the boundary conditions at r = R. The requirements of continuity of pressure and normal velocity give the following conditions:

$$\phi_1 = \phi_2 , \quad -e_1 \le z \le -d_1 \tag{22}$$

$$\phi_1 = \phi_3 , \quad -h_1 \le z \le -e_2 \tag{23}$$

$$\frac{\partial \phi_1}{\partial r} = \begin{cases} 0 & -d_1 < z < 0 \\ \dfrac{\partial \phi_2}{\partial r} & -e_1 < z < -d_1 \\ 0 & -e_2 < z < -e_1 \\ \dfrac{\partial \phi_3}{\partial r} & -h_1 < z < -e_2 \end{cases} \tag{24}$$

The boundary conditions above are satisfied over the z interval in a least square sense by multiplying each side of the boundary condition by a proper set of eigenfunctions and then by integrating them over the interval in question. Matching at r = R is achieved by the integrals following below, where the index k=1,2,.....

Boundary condition 1, Eq. (22):

$$\int_{-e_1}^{-d_1} \phi_1(R,z)\{\cos\beta_k(z+e_1)\}dz = \int_{-e_1}^{-d_1} \phi_2(R,z)\{\cos\beta_k(z+e_1)\}dz \tag{25}$$

Boundary condition 2, Eq. (23):

$$\int_{-h_1}^{-e_2} \phi_1(R,z)\{\cos\gamma_k(z+h_1)\}dz = \int_{-h_1}^{-e_2} \phi_3(R,z)\{\cos\gamma_k(z+h_1)\}dz \tag{26}$$

Boundary condition 3,Eq. (24):

$$\int_{-h_1}^{0} \frac{\partial \phi_1}{\partial r}\{\cos\beta_k(z+h_1)\}dz = \int_{-e_1}^{-d_1} \frac{\partial \phi_2}{\partial r}\{\cos\lambda_k(z+h_1)\}dz +$$

$$\int_{-h_1}^{-e_2} \frac{\partial \phi_3}{\partial r}\{\cos\beta_k(z+h_1)\}dz \tag{27}$$

Introduce the following integral functions

$$E(\alpha_n, \beta_k, h_\alpha, h_\beta, z_1, z_2) = \int_{z_1}^{z_2} \cos\alpha_n(z+h_\alpha)\cos\beta_k(z+h_\beta)dz \qquad (28)$$

$$N(\alpha_n, h_\alpha, z_1, z_2) = \int_{z_1}^{z_2} (\cos\alpha_n(z + h_\alpha))^2 dz \qquad (29)$$

where $\{\alpha_n,\ n = 1, 2,...\}$ and $\{\beta_k,\ k = 1, 2,...\}$ are two different sets of eigenvalues. Now, rewrite the boundary conditions, Eqs. (25) to (27), and introduce the integral functions (28) and (29). The following three sets of equations are then obtained:

Boundary condition 1:

$$\sum_{n=1}^{\infty} A_n E(\lambda_n,\beta_k,h_1,e_1,-e_1,-d_1) = P_{1k} + B_k N(\beta_k,e_1,-e_1,-d_1) \qquad (30)$$

where the component associated with the particular solution is given by

$$P_{1k} = \int_{-e_1}^{-d_1} \phi_{2p}^{(i)}(R,z) \cos\beta_k(z+e_1)\, dz \qquad (31)$$

Boundary condition 2:

$$\sum_{n=1}^{\infty} A_n E(\lambda_n,\gamma_k,h_1,h_1,-h_1,-e_2) = P_{2k} + C_k N(\gamma_k,h_1,-h_1,-e_2) \qquad (32)$$

where

$$P_{2k} = \int_{-h_1}^{-e_2} \phi_{3p}^{(i)}(R,z) \cos \gamma_k(z+h_1)\, dz \tag{33}$$

Boundary condition 3:

$$A_k D_k N(\lambda_k,h_1,-h_1,0) = P_{3k} + \sum_{n=1}^{\infty} \beta_n B_n \frac{I_o'(\beta_n R)}{I_o(\beta_n R)} E(\beta_n,\lambda_k,e_1,h_1,-e_1,-d_1) +$$

$$+ \sum_{n=1}^{\infty} \gamma_n C_n \frac{I_o'(\gamma_n R)}{I_o(\gamma_n R)} E(\gamma_n,\lambda_k,h_1,h_1,-h_1,-e_2) \tag{34}$$

where the component associated with the particular solution is given by

$$P_{3k} = \int_{-e_1}^{-d_1} \frac{\partial \phi_{2p}^{(i)}}{\partial r} \cos \lambda_k(z+h_1)\, dz + \int_{-h_1}^{-e_2} \frac{\partial \phi_{3p}^{(i)}}{\partial r} \cos \lambda_k(z+h_1)\, dz \tag{35}$$

and

$$D_k = \begin{cases} k\, H_o^{(1)'}(kR) / H_o^{(1)}(kR) & k = 1 \\ \lambda_k K_o'(\lambda_k R) / K_o(\lambda_k R) & k = 2,3,... \end{cases} \tag{36}$$

In order to find a solution, we must truncate the infinite series of orthogonal functions. Assume that N is the number of orthogonal functions considered. We then get a system of 3N complex equations and an equal number of unknown coefficients. Organizing the equations in matrices gives

$$\underline{\underline{S}}\, \underline{X} = \underline{F} \tag{37}$$

where

$$\underline{X} = -\frac{i g}{\omega} (A_1, A_2, .., A_N, B_1, B_2, .., B_N, C_1, C_2, .., C_N)^T$$

Let the elements in the system matrix be denoted by S_{ij} and the elements in the right hand side matrix by F_j, where i, j = 1, 2,..., 3N. The elements in the two matrices are given by the boundary conditions as follows below, with local indices n, k = 1, 2,..., N.

Boundary condition 1:

$$S_{kn} = E(\lambda_n, \beta_k, h_1, e_1, -e_1, -d_1) \tag{38a}$$

$$S_{k(N+k)} = -N(\beta_k, e_1, -e_1, -d_1) \tag{38b}$$

$$F_k = P_{1k} \tag{38c}$$

Boundary condition 2:

$$S_{(N+k)n} = E(\lambda_n, \gamma_k, h_1, h_1, -h_1, -e_2) \tag{38d}$$

$$S_{(N+k)(2N+k)} = -N(\gamma_k, h_1, -h_1, -e_2) \tag{38e}$$

$$F_{(N+k)} = P_{2k} \tag{38f}$$

Boundary condition 3:

$$S_{(2N+k)(N+n)} = -\beta_n \frac{I_o'(\beta_n R)}{I_o(\beta_n R)} E(\beta_n, \lambda_k, e_1, h_1, -e_1, -d_1) \tag{38g}$$

$$S_{(2N+k)(2N+n)} = -\gamma_n \frac{I_o'(\gamma_n R)}{I_o(\gamma_n R)} E(\gamma_n, \lambda_k, h_1, h_1, -h_1, -e_2) \tag{38h}$$

$$S_{(2N+k)k} = D_k N(\lambda_k, h_1, -h_1, 0) \tag{38i}$$

$$F_{(2N+k)} = P_{3k} \tag{38j}$$

Solving the complex system of equations gives the unknown coefficients in the orthogonal series and, thereby, also the potentials valid in each region.

The forces caused by the motion of the structure are calculated by integration of the dynamic pressure given by the Bernoulli equation. In order to be consistent with the linear formulation, the pressure is given by

$$p = -\rho \frac{\partial \Phi}{\partial t} = i\omega\rho\phi\, \zeta^{(i)} \tag{39}$$

where $\zeta^{(i)}$ is the motion of the oscillating body. The force at body j, caused by an oscillation of body i, can be written as one part proportional to the acceleration of body i and one part proportional to the velocity, as follows:

$$F^{(ij)} = - A^{(ij)}\zeta^{(i)} - B^{(ij)}\zeta^{(i)} \tag{40}$$

The quantities introduced, $A^{(ij)}$ and $B^{(ij)}$, are the added mass and potential damping respectively. The integration of the pressure over each body yields the following expressions for the hydrodynamic coefficients:

$$A^{(11)} + \frac{iB^{(11)}}{\omega} = 2\pi\rho\left[\frac{h_2^2R^2 - R^4/4}{4h_2} + \sum_{n=1}^{N} B_n \frac{(-1)^{n-1} R\, I_1(\beta_n R)}{\beta_n\, I_o(\beta_n R)}\right] \tag{41}$$

$$A^{(12)} + \frac{iB^{(12)}}{\omega} = 2\pi\rho\left[\sum_{n=1}^{N} C_n \frac{(-1)^{n-1} R\, I_1(\gamma_n R)}{\gamma_n\, I_o(\gamma_n R)} - B_n \frac{R\, I_1(\beta_n R)}{I_o(\beta_n R)\beta_n} \frac{R^4}{16h_2}\right] \tag{42}$$

$$A^{(21)} + \frac{iB^{(21)}}{\omega} = 2\pi\rho\left[\sum_{n=1}^{N} B_n \frac{(-1)^{n-1} R\, I_1(\beta_n R)}{\beta_n\, I_o(\beta_n R)} + \frac{R^4}{16h_2}\right] \tag{43}$$

$$A^{(22)} + \frac{iB^{(22)}}{\omega} = 2\pi\rho\left[\sum_{n=1}^{N} C_n \frac{(-1)^{n-1} R\, I_1(\gamma_n R)}{\gamma_n\, I_o(\gamma_n R)} - B_n \frac{R\, I_1(\beta_n R)}{I_o(\beta_n R)\beta_n} + \frac{R^2}{4}(h_3+h_2-\frac{R^2}{4h_2} - \frac{R^2}{4h_3})\right] \quad (44)$$

The hydrodynamic quantities given by the expressions above are the main results and will be presented in the next section.

4. NUMERICAL RESULTS

As an initial check of the result, a comparison is made between the present solution and a solution for a single buoy [7]. The solution for the single buoy is based on an approach[5] similar to that used in this paper. In the comparison the draught of the buoy to the water depth ratio $d_1 / h_1 = 0.25$, and the radius to the water depth ratio
$R / h_1 = 0.5$. In the solution given here the plate was kept close to the sea bottom
($d_2 / h_1 = 0$ and $h_3 / h_1 = 0.01$) in order to avoid influencing the added mass and damping of the oscillating buoy. The comparison is shown in Figure 3a- b. In the following figures and tables, the added mass is non-dimensionalized by the mass of the water displaced by a semi immersed sphere with the radius R, and the potential damping is non-dimensionalized by the same factor multiplied by the angular velocity ω, i.e.

$$a^{(ij)} = \frac{3A^{(ij)}}{2\pi R^3 \rho} \quad (46)$$

$$b^{(ij)} = \frac{3A^{(ij)}}{2\pi R^3 \rho\omega} \quad (47)$$

For the added mass the maximum relative deviation, between the present method and the single buoy is less than 1.5%. The agreement is even better when comparing the potential damping.

In Yeung[5] an approximative low frequency solution is presented. The approximation, which is reported to give reasonably accurate predictions
when $R/h_1 > 1$, is :

$$a^{(11)}(kR \to 0) = \frac{3}{4}\left[\frac{R}{4(h_1 - d_1)} - \frac{R}{h_1}(-\gamma + \ln 2 - \ln kR)\right] \qquad (47)$$

$$b^{(11)}(kR \to 0) = \frac{3\pi R}{8h_1}\left[1 + (kR)^2\left(\frac{\pi}{2} - \gamma + \ln 2 - \ln kR\right)\right]^{-1} \qquad (48)$$

where γ is the Euler constant ($\gamma \approx 0.5772$). Hence, it can be seen that the added mass at low frequency becomes logarithmic singular, while the damping approaches a constant value. In the range when the approximation is valid, the present method gives results in reasonable agreement with Eqs. (47) and (48) (See Table I).

Table I Comparison between the present method and Yeungs approximation for low frequency. $R/h_1 = 2$, $d_1/h_1 = 0$, $d_2/h_1 = 0$, $h_3/h_1 = 0.01$

	Yeung		Present Method	
kR	$a^{(11)}$	$b^{(11)}$	$a^{(11)}$	$b^{(11)}$
3.2e-4	12.62	2.356	12.84	2.356
3.2e-3	9.169	2.356	9.393	2.356
3.2e-2	5.715	2.344	5.929	2.347
3.1e-1	2.255	1.826	2.395	1.982

The truncation characteristics of the present solution are reasonable. Typically, in a wide frequency range, an increase from 10 terms in the series solutions to 50 terms gives a maximum relative deviation for $a^{(11)}$ of 11.2%. An increase from 20 to 50 terms yields a maximum relative deviation of 3.9%. Finally, an increase from 30 to 50 terms gives a maximum relative deviation of 0.5%.

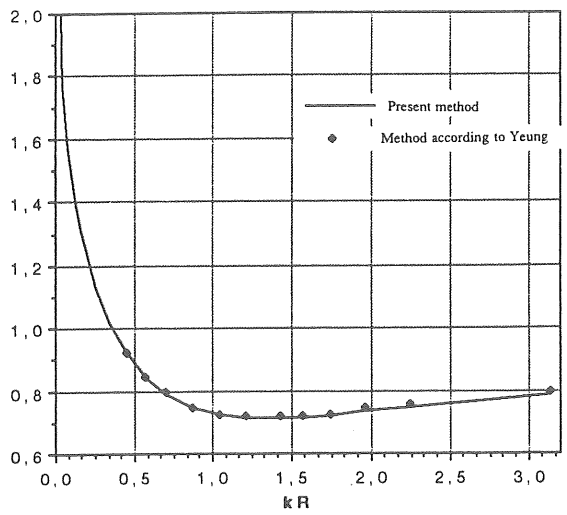

Figure 3a Coefficients of added mass for the buoy associated with vertical motion ($d_1/h_1 = 0.25$, $R/h_1 = 0.50$, $h_2/h_1 = 0.74$, $d_2/h_1 = 0$ and N=50). Comparison with the solution of a single floating cylinder.

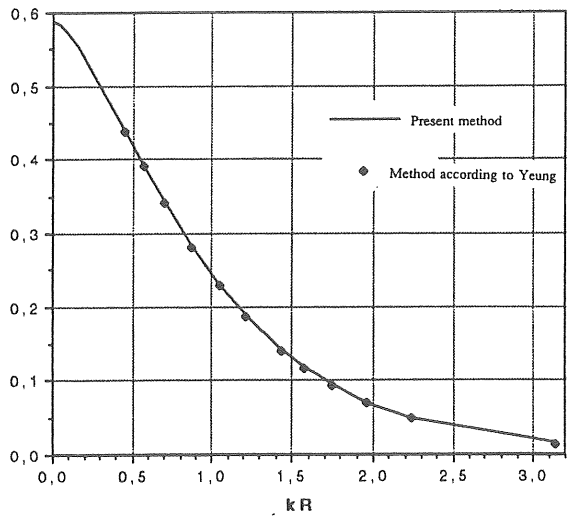

Figure 3b Coefficients of potential damping for the buoy associated with vertical motion ($d_1/h_1 = 0.25$, $R/h_1 = 0.50$, $h_2/h_1 = 0.74$, $d_2/h_1 = 0$ and N = 50). Comparison with the solution of a single floating cylinder.

The magnitude of the hydrodynamic coefficients of both the buoy and the plate, as a consequence of the motions of each one are shown in Figure 4a-d. The different curves show the different distances between the two bodies. The geometric configuration is $d_1 / h_1 = 0.1$, $R / h_1 = 0.2$ and $d_2 / h_1 = 0.1$. The distance between the two bodies varied as $h_2 / h_1 = 0.15$, 0.3 and 0.6.

It appears from Figure 4a and 4c that the added mass of the plate is greater than that of the buoy i.e. $a^{(11)} < a^{(22)}$. This is due to the fact that the plate is surrounded by the fluid while the buoy only has fluid on its under side. On the other hand, potential damping of the buoy is greater than that of the plate i.e. $b^{(11)} > b^{(22)}$, which is due to the fact that the submerged plate radiates fewer waves than the buoy. This was investigated numerically by integrating the pressure in phase with the velocity on the top face and bottom face of the plate. These integrated forces were found to be of the same magnitude but with opposite signs.

In the diagram it can also be seen that the added mass approaches a constant value when kR grows to infinity and the potential damping approaches zero. The asymptotic value of the added mass in infinitely deep water is given simply by $a^{(11)}(kR \to \infty) = \frac{2}{\pi}$, see Miles[8]. Due to the presence of the sea bottom and the submerged plate, the asymptotic added mass exceeds the infinitely deep water value.

Furthermore, from the numerical result it appears that $a^{(ij)} = a^{(ji)}$ and $b^{(ji)} = b^{(ij)}$, respectively. That these relations are valid can be shown with Green's theorem by applying it on the surfaces that surround the fluid domain (the wet surfaces of the buoy, the free surface of the water, the sea floor, and a surface that joins the free surface and the bottom surface) and the surface of the plate[9].

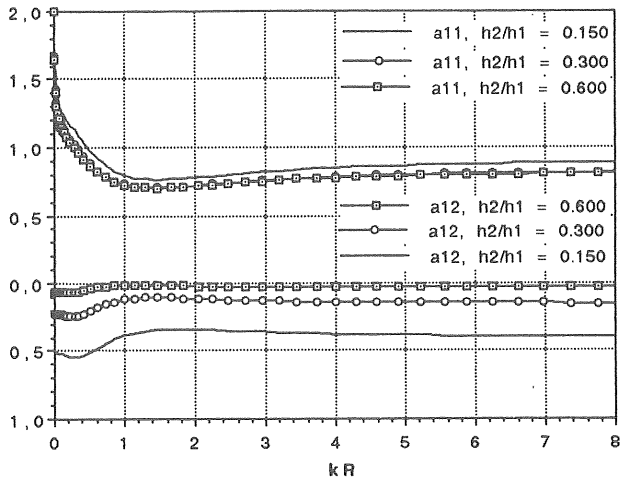

Figure 4a Added mass of the buoy and the plate as a consequence of the motion of the buoy.

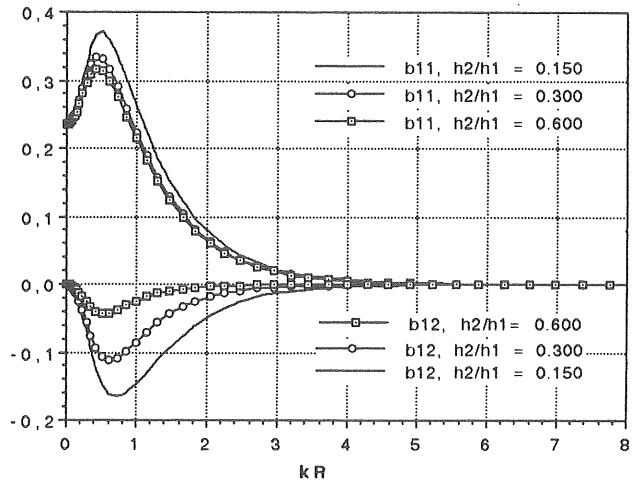

Figure 4b Potential damping of the buoy and the plate as a consequence of the motion of the buoy.

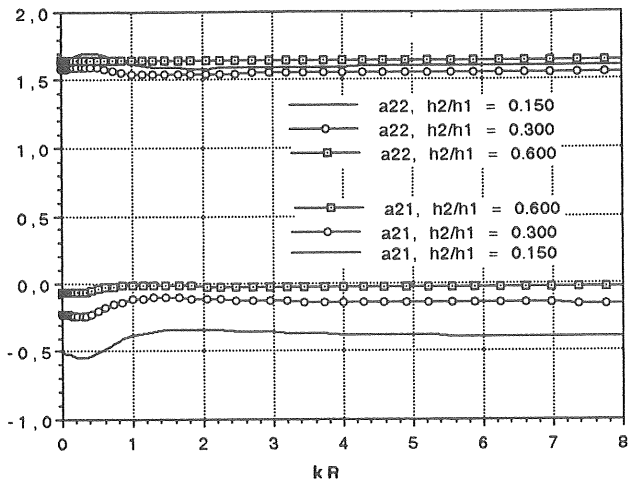

Figure 4c Added mass of the buoy and plate as a consequence of the motion of the plate.

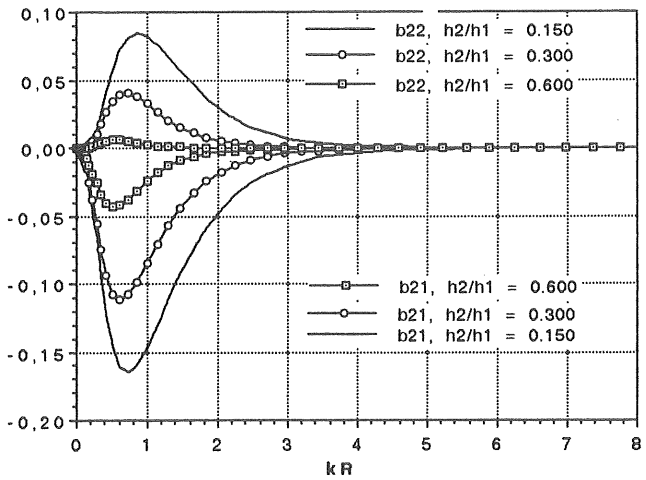

Figure 4d Potential damping of the buoy and the plate as a consequence of the motion of the plate.

If the plate oscillates close to the buoy or close to the sea floor, the added mass will grow to infinity as the distances h_2 and/or h_3 approach zero. This is also in agreement with the potential theory (the potential theory, however is simply a proper model for real conditions as long as $h_i / \delta > 1$ with $i = 2, 3$ and δ = the thickness of Stokes' boundary layer[10]).

It should be pointed out that some care must been taken when calculating the hydrodynamic coefficients for small values of h_2 and/or h_3. As h_2 and/or h_3 approach zero, the eigenvalues β_n and γ_n grow to infinity. If we calculate the coefficients in Eq.(25) we get:

$$\int_{-e_1}^{-d_1} \phi_1(R,z)\{\cos \beta_k(z+e_1)\}dz \sim \begin{cases} 1\lambda_n\left\{\sinh(h_1-d_1) - \sinh(h_1-e_1)\right\} & n = 1 \\ h_2^2 & n > 1 \end{cases} \quad (49)$$

$$\int_{-e_1}^{-d_1} \phi_2^{Hom}(R,z)\{\cos \beta_k(z+e_1)\}dz = \begin{cases} h_2 & n = 1 \\ \frac{h_2}{2}\left\{\frac{\sin 2\pi n(n-1)}{2\pi(n-1)} + 1\right\} & n > 1 \end{cases} \quad (50)$$

$$\int_{-e_1}^{-d_1} \phi_2^{Part}(R,z)\{\cos \beta_k(z+e_1)\}dz = \begin{cases} -R^2/4 + h_2^2/6 & n=1 \\ \frac{h_2^2(-1)^{n-1}}{(n-1)\pi^2} & n>1 \end{cases} \quad (51)$$

If we solve the matrices (37) for small values of h_2, the terms B_n will approach

$$B_n \begin{cases} = R^2/4h_2 & n = 1 \\ \sim h_2 & n > 1 \end{cases} \quad (52)$$

and terms of higher order than 1 can be omitted for small values of h_2. If we substitute this relation into Eq.(41) and calculate the added mass we get:

$$A^{(11)} = 2\pi\rho\left[\frac{h_2^2R^2}{4} - \frac{R^4}{16h_2} + \frac{R^4}{8h_2}\right] = \frac{\pi\rho R^4}{8h_2} \quad (53)$$

In a similar way we get:

$$A^{(12)} = \frac{\pi\rho R^4}{8h_2} \tag{54}$$

$$A^{(21)} = \frac{\pi\rho R^4}{8h_2} \tag{55}$$

$$A^{(22)} = \frac{\pi\rho R^4}{8}\left[\frac{1}{h_2} + \frac{1}{h_3}\right] \tag{56}$$

When either h_2 or h_3 approach zero, one gets the same result as in Bergdahl et al.[11]

Where the added mass was estimated by calculating directly the kinetic energy of the fluid in the narrow space between the bottom of a circular platform and the sea floor under the assumption of uniform, radial flow. A comparison was made between the general formulation (Eqs. 41 - 44) and the narrow spaced approximation

(Eqs. 53 - 56) for decreasing value of the ratio h_2 / h_1.

Table II

Added mass as a consequence of diminishing h_2/h_1 where $R/h_1 = 0.2$, $d_1/h_1 = d_2/h_1 = 0.2$, $N = 30$ and $kR = 3.19\ 10^{-3}$

h_2/h_1	$a^{(11)}$	$a^{(12)}$	$a^{(22)}$	$a^{(21)}$	$3R/16h_2$
0.01000	5.3656	-4.5863	-4.2563	5.3499	3.7500
0.00100	39.099	-38.291	-38.291	39.081	37.500
0.00010	376.60	-375.79	-375.79	376.59	375.00
0.00001	3751.6	-3750.8	-3750.8	3751.6	3750.0

The difference between $a^{(11)}$ and $a^{(12)}$ when $h_2 / h_1 = 0.01$ is mainly caused by the contribution from the potential ϕ_3 to the added mass $a^{(12)}$. If we separate the added mass, $a^{(12)}$, into two parts, one for the upper side and one for the lower side of the submerged plate we get:

$$a^{(12)}_{\text{upper side}} = -5.3292 \text{ with } h_2 / h_1 = 0.01$$

$$a^{(12)}_{\text{upper side}} = -3751.6 \text{ with } h_2 / h_1 = 0.00001$$

The calculations indicates that when $h_2/h_1 \to 0$ then $|a^{(11)}| = |a^{(12)}_{\text{upper side}}|$.

5. CONCLUSIONS

This study treats the radiation problem of a two-body system, where one of the bodies is submerged and the other is floating. The problem is solved by using the method of eigenfunction expansions. There is reasonable agreement with existing solutions for a single cylinder. The present solution converges acceptably when including 30 terms in the eigenfunction expansions (in the cases tested the relative deviation is less than 0.5% between a solution truncated at 30 terms and one truncated at 50 terms).

A narrow space analysis is performed. The formulas derived are in agreement with formulas derived directly from energy relations.

ACKNOWLEDGEMENT

This research has been carried out at the Dept. of Hydraulics, Chalmers University of Technology, Sweden. Financial support was provided by the National Energy Administration, Sweden (STEV).

REFERENCES

1 Hagerman, G.W., Wave energy resource and technology assessment for coastal North Carolina. SEASUN Power System, Alexandria, Virgina, USA 1988.

2 McIver, P., Wave forces on adjacent floating bridges. Applied Ocean Research, 1981, Vol.3, No.3.

3 Wu, J. and Philip, L.-F., Interactions of obliquely incident water waves with two vertical obstacles. Applied Ocean Research, 1988, Vol.10, No.2

4 Johansson, M., Barrier-type breakwaters - Transmission, reflection and forces. Ph.D. Thesis, Report A:19, Dept. Hydraulics, Chalmers University of Technology, 1989.

5 Yeung, R.W., Added mass and damping of a vertical cylinder in finite-depth waters. Applied Ocean Research, 1981, Vol. 3, No. 3.

6 Miao, G.P. and Liu, Y.Z., Hydrodynamic coefficients of a column with footing in finite-depth waters. Proc. 3rd Int. Symp. Offshore Mechanics and Arctic Engineering, 1984, Vol.I, pp. 199-205.

7 Johansson, M., Transient motion of large floating structures. Lic. Eng. Thesis, Report A:14, Dept of Hydraulics, Chalmers University of Technology, 1987.

8 Miles, J.W., On surface-wave forcing by a circular disk, J. Fluid Mechanics, 1987, Vol 175, pp 97-108.

9 Srokosz, M.A. and Evans, D.V., A theory for wave-power absorption by two independently oscillating bodies, 1979, Vol. 90, part 2, pp. 337-362.

10 Mei Chiang C., Effects on narrow gap between a bottom- seated structure and the sea-floor. Applied Ocean Research, 1987, vol. No. 1.

11 Bergdahl, L. and Pålsson, I., Marine operations of detachable production platform, The 10th International Conference on Port and Ocean Engineering under Arctic Conditions, 1989.

Forces on a wave-energy module

LARRY BERGGREN and LARS BERGDAHL
Dept. of Hydraulics, Chalmers University of Technology
412 96 Göteborg, Sweden

Mathematical models for the calculation of wave forces added mass and radiation damping of a wave-energy module are developed in order to assess the energy take-out. The module consists
If a buoy connected to a submerged plate by a hose pump.

In the models presented the buoy and the submerged plate are idealized as two cylinders of equal radius.The method presented is founded on matched eigenfunction expansion. Comparisons with other solutions are presented and the agreement is shown to be satisfactory. The models developed are computer efficient and will be used in an optimization procedure for a wave climate.

1 INTRODUCTION

One of the wave-energy conversion devices tested in Sweden is the hose pump concept developed by Götaverken Energy [1, 2]. The concept consists of a buoy, riding in the waves, connected to a submerged plate by an elastomeric hose. The submerged plate is moored to the sea floor. The elastomeric hose acts as a pump that is driven by the relative heaving motion between the buoy and the submerged plate. (See Fig 1)

During the passage of a wave crest, the buoy heaves up, stretching the hose. The helical pattern of steel reinforcing wires in the hose wall causes it to constrict as it is stretched, thereby reducing its internal volume. This forces seawater out of the hose pump, through a check valve, and into a collecting line to a turbine. After the wave crest has passed and the buoy drops down into the succeeding trough, the hose returns to its original length, restoring its diameter to its unstretched value. This increase in internal volume draws water into the the hose through another check valve, which is open to the sea.

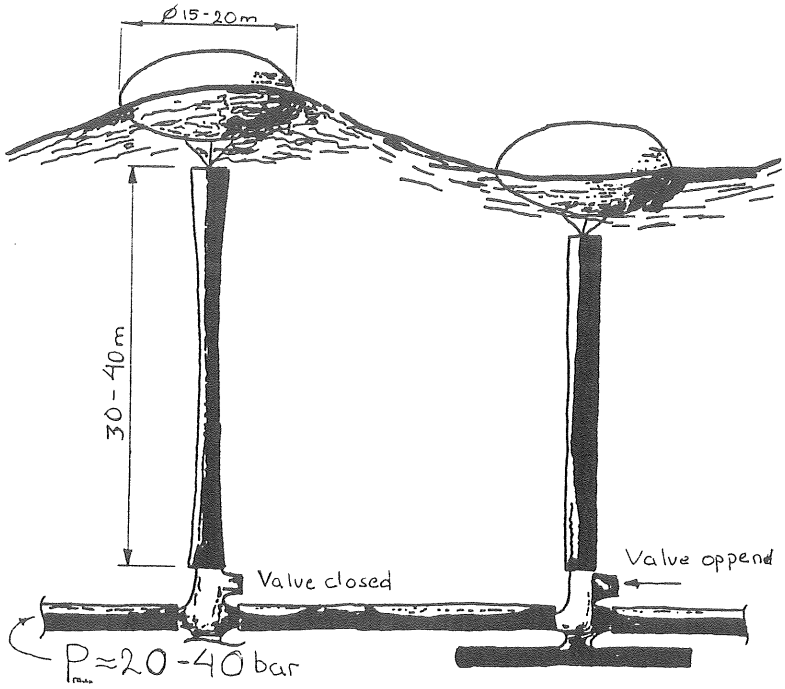

Figure 1 Outline drawing of two Wave-Energy modules.

In this paper a hydrodynamic model for such a wave energy module is presented. In the model presented the buoy and the submerged plate are idealized as two cylinders of equal radius, the hose pump as a linear spring and damper in parallel, and the mooring as a weak linear spring. The ambient fluid is regarded as incompressible, irrotational and nonviscous. For this particular case, the wave forces and hydrodynamic properties of the device can be solved by the method of matched eigenfunction expansion.

2 EQUATIONS OF MOTION OF THE WAVE ENERGY MODULE

With nomenclature according to Fig. 2 the equations of motion of the buoy and the submerged plate can be written

$$\begin{cases} m_b\ddot{z}_b + c_1(\dot{z}_b-\dot{z}_p) + k_1(z_b-z_p) + dz_b = F_b \\ m_p\ddot{z}_p + c_1(\dot{z}_p-\dot{z}_b) + k_1(z_p-z_b) + k_2 z_p = F_p \end{cases} \quad (1)$$

with
- b = buoy
- p = plate
- m_i = the mass of body i
- c_i = the damping coefficient
- k_i = the spring stiffness for spring i
- F_i = the forces on body i caused by the incident waves

To solve this problem, we first have to calculate the forces that act upon the two bodies, F_b and F_p. One way to determine F_b and F_p is to separate the problem into two parts, a diffraction problem and a radiation problem. In the diffraction problem, we calculate the wave exciting forces, ${}_dF_b$ and ${}_dF_p$, with the buoy and the plate kept in a fixed position. The forces set the buoy and the plate into motion, which results in radiated waves and reaction forces from the water. The reaction forces are solved in the radiation problem. When solving the radiation problem, we give the buoy and the plate, one at the time, a forced harmonic vertical motion and calculate the hydrodynamic coefficients, i.e. added mass, a^{ij}, and potential damping, b^{ij}. This means that we will get two sets of values of added mass and potential damping on each body. When the buoy is given a forced motion while the plate is kept in a fixed position, a reaction force acts not only on the buoy but on the plate as well, i.e. we calculate added mass and potential damping, as a consequence of the motion of the buoy on both the buoy and the plate. When this is done we make the same calculation again but now the plate is given a forced motion and the buoy is kept in a fixed position. The force at body j caused by an oscillation of body i can be written as one part proportional to the acceleration and one part to the velocity as follows:

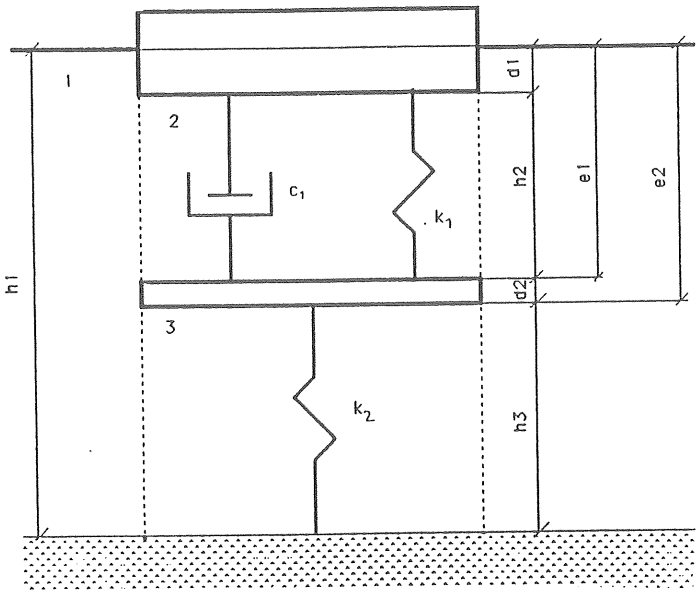

Figure 2 Geometrical properties of the wave energy module and definition of fluid subdomains.

$$F^{ij} = -a^{ij}\, z_i - b^{ij}\, z_i \tag{2}$$

and the total forces that act on the buoy and plate due to the radiation are

$$\begin{cases} {}_rF_b = -(a^{11}\,\ddot{z}_b + b^{11}\,\dot{z}_b + a^{12}\,\ddot{z}_p + b^{12}\,\dot{z}_p) \\ {}_rF_m = -(a^{22}\,\ddot{z}_p + b^{22}\,\dot{z}_p + a^{21}\,\ddot{z}_b + b^{21}\,\dot{z}_b) \end{cases} \tag{3}$$

and when the wave exciting forces are included we get

$$\begin{cases} F_b = {}_dF_b - (a^{11}\,\ddot{z}_b + b^{11}\,\dot{z}_b + a^{12}\,\ddot{z}_p + b^{12}\,\dot{z}_p) \\ F_m = {}_dF_p - (a^{22}\,\ddot{z}_p + b^{22}\,\dot{z}_p + a^{21}\,\ddot{z}_b + b^{21}\,\dot{z}_b) \end{cases} \tag{4}$$

If the forces and the motions varies periodically with the time we get

$$\begin{cases} z_i = Z_i e^{j\omega} \\ \dot{z}_i = j\omega Z_i e^{j\omega t} \\ \ddot{z}_i = -\omega^2 Z_i e^{j\omega t} \\ {}_dF_i = {}_df_i e^{j\omega t} \end{cases} \tag{5}$$

where

$j = \sqrt{-1}$, ω = angular frequency and t = time

The only problems that remain to be solved are the wave exciting forces, the added mass and the potential damping.

3 CALCULATIONS OF THE WAVE EXCITING FORCES

If the amplitude of the incident wave is denoted η, then the flow is suitably described by the velocity potential $Re\{-j\ \omega\ \eta\ \phi(r, z)e^{-j\omega t}\}$ where the spatial part of the velocity potential ϕ is governed by the following boundary-value problem:

$$\frac{\partial^2\phi}{\partial z^2} + \frac{1}{r}\frac{\partial}{\partial r}\left(r\frac{\partial\phi}{\partial r}\right) = 0 \qquad \text{(everywhere)} \tag{6}$$

$$\frac{\partial\phi}{\partial z} = 0 \qquad (z = -h_1) \tag{7}$$

$$\frac{\partial\phi}{\partial z} = 0 \qquad (z = -d_1,\ r < R) \tag{8}$$

$$\frac{\partial\phi}{\partial z} = 0 \qquad (z = -e_1,\ r < R) \tag{9}$$

$$\frac{\partial\phi}{\partial z} = 0 \qquad (z = -e_2,\ r < R) \tag{10}$$

$$\frac{\partial \phi}{\partial r} = 0 \qquad (-d_1 < z < 0,\ r = R) \tag{11}$$

$$\frac{\partial \phi}{\partial r} = \left(-\frac{1}{2r} + ik\right)\phi \qquad (r \to \infty) \tag{12}$$

$$\frac{\partial \phi}{\partial r} = 0 \qquad (-e_2 < z < -e_1,\ r = R) \tag{13}$$

$$\frac{\partial \phi}{\partial z} - \frac{\omega^2}{g}\phi = 0 \qquad (z = 0,\ r \geq a) \tag{14}$$

$$\phi(\theta) = \phi(-\theta) \tag{15}$$

where k is the wave number. The potential of the incident wave is expressed as

$$\phi_i = \phi_i e^{j(kx-\omega t)} = \frac{jgh_1}{2\omega}\frac{\cosh\ k(z+h_1)}{\cosh\ kh_1} e^{j(kx-\omega t)} \tag{16}$$

If $x = r\cos\theta$ we can use a well known expression:

$$e^{jkr\cos\theta} = \sum_{n=0}^{\infty} \varepsilon_n j^n J_n(kr)\cos n\theta \tag{17}$$

Then Eq. (16) becomes:

$$\phi_i = \frac{jgh_1}{2\omega}\frac{\cosh\ k(z+h_1)}{\cosh\ kh_1}\sum_{n=0}^{\infty} \varepsilon_n j^n J_n(kr)\cos n\theta \tag{18}$$

where J_n is the Bessel function of the first kind and order n, $\varepsilon_n = \begin{cases} 1 & n = 0 \\ 2 & n = 1, 2,.. \end{cases}$

In the solution procedure the fluid domain is divided into three sub domains as indicated in Figure 2. The method of separation of variables is applied in each sub domain in order to obtain expressions for the unknown function, i.e. the velocity potential. Expressions valid in each sub domain are obtained as infinite series of

orthogonal functions. These expressions are developed to satisfy all boundary conditions except at the boundaries joining the sub domains, i.e. at r = R. The next step is to determine a number of unknown coefficients in the series. This is done by imposing the condition of continuity of pressure and normal velocity at r = R. Mathematically this is fulfilled by matching the potentials and the normal derivatives of the potentials respectively.

The formulation starts from the potentials developed independently in each sub domain. Applying the method of separation of variables gives the spatial potentials in each sub domain expressed in terms of orthogonal series. In sub domain 1 the potential is

$$\phi_1 = \sum_{n=0}^{\infty} \sum_{m=0}^{\infty} A_{nm} \cos\lambda_m(z+h_1) \frac{R_n(\lambda_m r)}{R_n(\lambda_m R)} \qquad (19)$$

where the eigenvalues are given by

$\lambda_1 = -ik$ where k is the wave number

$k \tanh kh_1 = \omega^2/g$ $\quad m = 0$ (20 a)

$\lambda_m \tan \lambda_m h_1 = -\omega^2/g$ $\quad m = 1, 2..$ (20 b)

and the radial function R_n is given by

$R_1(\lambda_0 r) = H_n^{(1)}(i\lambda_0 r) = H_n^{(1)}(kr)$ $\quad m = 0$ (21 a)

$R_n(\lambda_m r) = K_n(\lambda_m r)$ $\quad m = 1, 2..$ (21 b)

where $H_n^{(1)}$ is the Hankel function of first kind and n:th order, and K_n is the modified Bessel function of second kind and n:th order.

In sub domains 2 and 3 the potential and corresponding eigenvalues are

$$\phi_{2d} = \sum_{n=0}^{\infty}\sum_{m=0}^{\infty} B_{nm}\cos\beta_m(z+e_1)\frac{I_n(\beta_m r)}{I_n(\beta_m R)}\cos n\theta \quad \beta_m = m\pi/h_2 \tag{22}$$

$$\phi_{3d} = \sum_{n=0}^{\infty}\sum_{m=0}^{\infty} C_{nm}\cos\gamma_m(z+e_1)\frac{I_n(\gamma_m r)}{I_n(\gamma_m R)}\cos n\theta \quad \gamma_m = m\pi/h_1 \tag{23}$$

The remaining problem is to determine the unknown coefficients A_{nm}, B_{nm} and C_{nm}. We now use the three boundary conditions which state, r = R, continuity of pressure and normal velocity, mathematically:

$$\phi_i + \phi_{1d} = \phi_{2d}, \qquad -e_1 \le z \le -d_1 \tag{24}$$

$$\phi_i + \phi_{1d} = \phi_{3d}, \qquad -h_1 \le z \le -e_2 \tag{25}$$

$$\frac{\partial(\phi_i+\phi_{1d})}{\partial r} = \begin{cases} 0 & -d_1<z<0 \\ \dfrac{\partial\phi_{2d}}{\partial r} & -e_1<z<-d_1 \\ 0 & -e_2<z<-e_1 \\ \dfrac{\partial\phi_{3d}}{\partial r} & -h_1<z<-e_2 \end{cases} \tag{26}$$

The boundary conditions above are satisfied in a least square sense by multiplying each side of the boundary condition with a proper set of eigenfunctions and then integrating over the interval in question. The matching at r = R is achieved by the integrals following below, with k = 1, 2.. and $\phi_o = \phi_i + \phi_{1d}$.

Boundary condition 1, Eq. (24), becomes

$$\int_{-e_1}^{-d_1} \phi_o(R, z)\{\cos\beta_k(z + e_1)\}dz = \int_{-e_1}^{-d_1} \phi_{2d}(R, z)\{\cos\beta_k(z+e_1)\}dz \tag{27}$$

and boundary condition 2, Eq. (25),

$$\int_{-h_1}^{-e_2} \phi_o(R, z)\{\cos \gamma_k(z + h_1)\}dz = \int_{-h_1}^{-e_2} \phi_{3d}(R, z)\{\cos \gamma_k(z+h_1)\}dz \tag{28}$$

and finally, boundary 3, Eq. (26), becomes

$$\int_{-h_1}^{0} \frac{\partial \phi_o}{\partial r}\{\cos \lambda_k(z + h_1)\}dz = \int_{-e_1}^{-e_2} \frac{\partial \phi_{2d}}{\partial r}\{\cos \lambda_k(z + h_1)\}dz +$$

$$\int_{-h_1}^{-e_2} \frac{\partial \phi_{3d}}{\partial r}\{\cos \lambda_k(z + h_1)\}dz \tag{29}$$

Next the following integral functions are introduced

$$E(\alpha_m, \mu_k, h_\alpha, h_\mu, z_1, z_2) = \int_{z_1}^{z} \cos \alpha_m(z + h_\alpha) \cos \mu_k(z+h_\mu)dz \tag{30}$$

$$N(\alpha_m, h_\alpha, z_1, z_2) = \int_{z_1}^{z_2} (\cos \alpha_m(z + h_\alpha))^2 dz \tag{31}$$

where $\{\alpha_m, m = 1, 2,...\}$ and $\{\mu_k, k = 1, 2,...\}$ are two different sets of eigenvalues for λ_m, β_m or γ_m.

In order to find a numerical expression we have to truncate the series (19), (22) and (23). The eigenvalues λ_m, β_m and γ_m are truncated at M, and cos $n\theta$ at N. This means that for each truncation term of n we have two different sets eigenvalues, α_m and μ_k. Now, rewriting the boundary conditions, Eqs. (27) to (29), introducing the functions (30) and (31) and organizing all functions in matrices for each n gives

$$\underline{\underline{{}_nS}}\ \underline{{}_nX} = \underline{{}_nF} \tag{32}$$

where

$$ {}_n\underline{X} = (A_{n1},\ldots,A_{nM},B_{n1},\ldots,B_{nM},C_{n1},\ldots,C_{nM})^T \tag{33} $$

The boundary condition can be rewritten and put into matrices:
for boundary condition 1

$$ {}_nS(m, m) = E(\lambda_m, \beta_k, h_1, e_1, d_1, e_1) \tag{34a} $$

$$ {}_nS(m, M + m) = N(\beta_m, e_1, -d_1, -e_1) \tag{34b} $$

$$ {}_nF(m) = J_n(\lambda_0 R)\delta_n E(\lambda_m, \beta_k, h_1, e_1, -d_1, -e_1) \tag{34c} $$

for boundary condition 2

$$ {}_nS(M + m, m) = E(\lambda_m, \gamma_k, h_1, h_1, -e_2, -h_1) \tag{35a} $$

$$ {}_nS(M + m, 2M + m) = N(\gamma_m, h_1, -e_2, -h_1) \tag{35b} $$

$$ {}_nF(M + m) = J_n(\lambda_0 R)\delta_n E(\lambda_m, \gamma_k, h_1, h_1, -e_2, -h_1) \tag{35c} $$

for boundary condition

$$ {}_nS(2M + m, m) = \eta(\lambda)\, N(\lambda_m, h_1, 0, -h_1) \tag{36a} $$

$$ {}_nS(2M + m, M + m) = \eta(\beta)\, E(\beta_m, \lambda_k, e_1, h_1, -d_1, -e_1) \tag{36b} $$

$$ {}_nS(2M + m, 2M + m) = \eta(\gamma)\, E(\gamma_m, \lambda_k, h_1, h_1, -e_2, -h_1) \tag{36c} $$

$$ {}_nF(2M + m) = \delta_n(-\lambda_0 J_{n-1}(\lambda_o R)+\frac{n}{R} J_n(\lambda_o R))\, E(\lambda_0, \lambda_k, h_1, e_1, d_1, e_1) \tag{36d} $$

$$ \delta_n = \begin{cases} \dfrac{j\, g h_1}{2\omega \cosh \lambda_0 h_1} & n = 0 \\ \dfrac{j^{(n+1)} g h_1}{\omega \cosh \lambda_0 h_1} & n = 1, 2.. \end{cases} \tag{37} $$

$$\eta(\lambda) = \begin{cases} \dfrac{-\lambda_0 H_{n-1}^{1}(\lambda_0 R)}{H_n^{1}(\lambda_0 R)} + \dfrac{n}{R} & m = 0 \\ \dfrac{-\lambda_m K_{n-1}^{1}(\lambda_m R)}{K_n^{1}(\lambda_m R)} + \dfrac{n}{R} & m = 1, 2,. \end{cases} \tag{38}$$

$$\eta(\beta) = \frac{\beta_m I_{n-1}(\beta_m R)}{I_n(\beta_m R)} + \frac{n}{R} \tag{39}$$

$$\eta(\gamma) = \frac{\gamma_m I_{n-1}(\gamma_m R)}{I_n(\gamma_m R)} + \frac{n}{R} \tag{40}$$

The unknown coefficients can now be calculated and also finally, the wave exciting forces. This is done by integrating the the potential over the surface:

$${}_dF_b = -j\rho\omega \iint_S n_z \phi_2 ds \tag{41}$$

where S is the surface and n_z the normal pointing out from the body:

$${}_dF_b = -j2\pi\rho\omega \sum_{m=0}^{M} B_{0m} \cos(\beta_m h_2) \frac{R}{\beta_m} \frac{I_1(\beta_m R)}{I_0(\beta_m R)} \tag{42}$$

In a similar way the forces on the plate is calculated :

$${}_dF_p = -j2\pi\rho\omega \sum_{m=0}^{M} \left[C_{0m} \cos(\gamma_m h_3) \frac{R}{\gamma_m} \frac{I_1(\gamma_m R)}{I_0(\gamma_m R)} - B_{0m} \frac{R}{\beta_m} \frac{I_1(\beta_m R)}{I_0(\beta_m R)} \right] \tag{43}$$

4 CALCULATION OF THE HYDRODYNAMIC COEFFICIENTS

When calculating the added mass and potential damping the solution procedures are very much alike those presented in the previous chapter, but there are some changes in the boundary condition, namely:

$$\frac{\partial \phi}{\partial z} = 1 \qquad (z=-d_1,\ r<R) \tag{44}$$

$$\frac{\partial \phi}{\partial z} = 0 \qquad (z=-e_1,\ r<R) \tag{45}$$

$$\frac{\partial \phi}{\partial z} = 0 \qquad (z=-e_2,\ r<R) \tag{46}$$

$$\frac{\partial \phi}{\partial z} = 0 \qquad (z=-d_1,\ r<R) \tag{47}$$

$$\frac{\partial \phi}{\partial z} = 1 \qquad (z=-e_1,\ r<R) \tag{48}$$

$$\frac{\partial \phi}{\partial z} = 1 \qquad (z=-e_2,\ r<R) \tag{49}$$

The equations (44) - (46) concern the case when the buoy is forced into motion and equations (47) - (49) the case when the plate is forced into motion. Since this problem is two-dimensional is radially symmetric boundary condition (15) is unnecessary. Boundary condition (24)-(26) at r=R will also change to:

$$\phi_{1r} = \phi_{2r}\ ,\ -e_1 \le z \le -d_1 \tag{50}$$

$$\phi_{1r} = \phi_{3r}\ ,\ -h_1 \le z \le -e_2 \tag{51}$$

$$\frac{\partial \phi_{1r}}{\partial r} = \begin{cases} 0 & -d_1 < z < 0 \\ \dfrac{\partial \phi_{2r}}{\partial r} & -e_1 < z < -d_1 \\ 0 & -e_2 < z < -e_1 \\ \dfrac{\partial \phi_{3r}}{\partial r} & -h_1 < z < -e_2 \end{cases} \tag{52}$$

due to the fact that there is no any incident wave. The F vector will instead be replaced by the particular solution we get when solving the inhomogeneous part of the boundary conditions (44) and (48), (49) respectively. The procedure is more elaborately described in [3]. After calculating the unknown coefficients in the same way as above we can calculate the hydrodynamic coefficients as

$$a^{11} + \frac{ib^{11}}{\omega} = 2\pi\rho\left[\frac{h_2^2R^2 - R^4/4}{4h_2} + \sum_{m=0}^{M} B_m \frac{(-1)^m R\, I_1(\beta_m R)}{\beta_m I_o(\beta_m R)}\right] \tag{53}$$

$$a^{12} + \frac{ib^{12}}{\omega} = 2\pi\rho\left[\sum_{m=0}^{M} C_m \frac{(-1)^m R\, I_1(\gamma_m R)}{\gamma_m I_o(\gamma_m R)} - B_m \frac{R\, I_1(\beta_m R)}{I_o(\beta_m R)\beta_m} + \frac{R^4}{16h_2}\right] \tag{54}$$

$$a^{21} + \frac{ib^{21}}{\omega} = 2\pi\rho\left[\sum_{m=0}^{M} B_m \frac{(-1)^m R\, I_1(\beta_m R)}{\beta_m I_o(\beta_m R)} + \frac{R^4}{16h_2}\right] \tag{55}$$

$$a^{22} + \frac{ib^{22}}{\omega} = 2\pi\rho\left[\sum_{n=0}^{M} C_m \frac{(-1)^m R\, I_1(\gamma_m R)}{\gamma_m I_o(\gamma_m R)} - B_n \frac{R\, I_1(\beta_m R)}{I_o(\beta_m R)\beta_m} + \frac{R^2}{4}(h_3 + h_2 - \frac{R^2}{4h_2} - \frac{R^2}{4h_3})\right] \tag{56}$$

5 RESULTS

When validating the program a comparison is made between the present solution and two different solutions of a single buoy. One of the solutions of the single buoy is based on a similar approach as in this paper [4]. The second one is based on a sink-source solution, Wadif,[5]. In the comparison the water depth is h_1 = 100m, the draught of the buoy d_1 = 25m, and the radius R = 50m. In the comparison the submerged plate in the present solution was kept close to the sea-bottom in order not to influence the diffraction force, the added mass and the potential damping of the buoy. The comparison is shown in figure 3a-d. The values given in the figures are non-dimensionalized, the diffraction force by the buoyancy force, the added mass by the mass of half a sphere of radius R and the radiation damping by this half sphere times the angular frequency ω.

The maximum relative deviation, for the diffraction force is less than 5.5% for the amplitude and 3.3% for the phase angles. In the radiation case, the maximum relative deviation for added mass is less than 4.5% (kR = 3.2) and a comparison between the present method and a single body gives a deviation less than 1.5%. The agreement is even better when comparing the potential damping, except when the comparison is made between the present solution and

Wadif for kR = 3.2 wich gives a relative deviation of 14%. The absolute deviation, however, is small.

One can also see in figure 3a that the ${}_dF_b$ is approaching 1, as expected, when the angular frequency is approaching zero i.e. the force will be equal to the buoyancy force. It is also evident that the force on the plate is approaching zero, as it should, when the angular frequency is approaching zero.

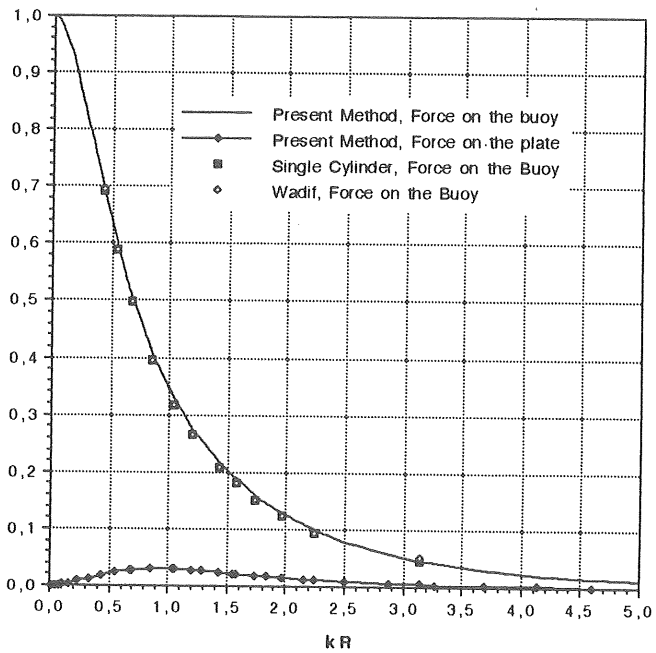

Figure 3a Amplitudes of the wave exciting forces for the buoy and submerged plate (h_1 = 110.0, d_1 = 25.0, R = 50.0, h_2 = 100.0, d_2 = 0.0). Comparison with the solution of a single floating cylinder.

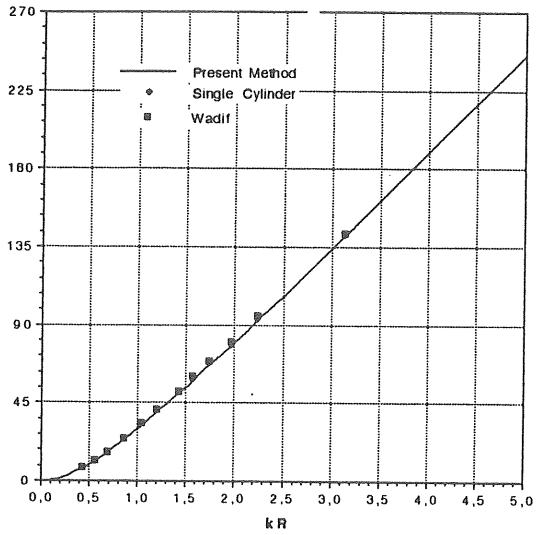

Figure 3b Phase angles (deg) of the wave exciting forces for the buoy and the submerged plate (h_1 = 110.0, d_1 = 25.0, R = 50.0, h_2 = 100.0, d_2 = 0.0). Comparison with the solution of a single floating cylinder.

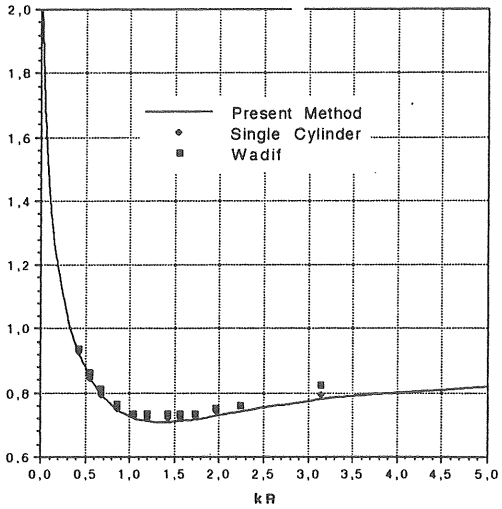

Figure 3c Coefficients of added mass for the buoy associated with vertical motion (h_1 = 100.0, d_1 = 25.0, R = 50.0, h_2 = 74.0, d_2 = 0.0 and N=50). Comparison with the solution of a single floating cylinder.

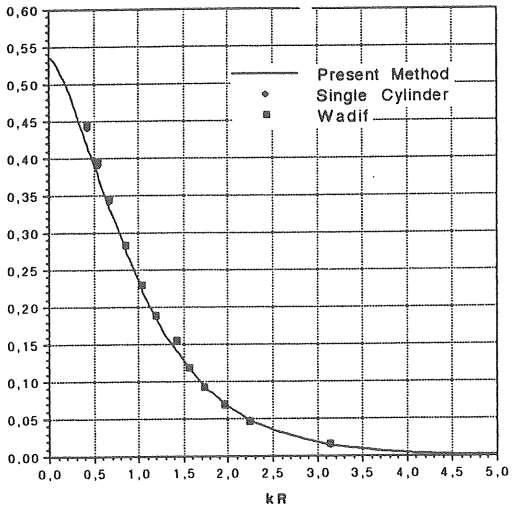

Figure 3d Coefficients of potential damping for the buoy associated with vertical motion (h_1 = 100.0, d_1 = 25.0, R = 50.0, h_2 = 74.0, d_2 = 0.0 and N = 50). Comparison with the solution of a single floating cylinder.

REFERENCES

[1] George Hagerman: Wave energy resource and technology assessment for coastal North Carolina. SEASUN Power System, Alexandria, Virginia, 1988.

[2] G. Svensson and R. Hardell: En svensk vågkraftidé. Energiforskningsnämnden. EFN-rapport nr 12, Sweden 1985 (A Swedish wave power idea)

[3] Larry Berggren and Mickey Johansson: Hydrodynamic coefficients of a wave energy device consisting of a buoy and a submerged plate. (Appendix A of this report.

[4] Mickey Johansson: Transient Motions of Large Floating Structures. Report Series A:14, Department of Hydraulics, Chalmers University of Technology, Göteborg, Sweden 1986.

[5] O.M. Faltinsen and F.C. Michelsen: Motion of large structures in waves with zero Froude number, Proc. Marine Vehicles in Waves Symp, 1975.

CHALMERS TEKNISKA HÖGSKOLA
Institutionen för vattenbyggnad

Report Series A

A:1 Bergdahl, L.: Physics of ice and snow as affects thermal pressure. 1977.

A:2 Bergdahl, L.: Thermal ice pressure in lake ice covers. 1978.

A:3 Häggström, S.: Surface Discharge of Cooling Water. Effects of Distortion in Model Investigations. 1978.

A:4 Sellgren, A.: Slurry Transportation of Ores and Industrial Minerals in a Vertical Pipe by Centrifugal Pumps. 1978.

A:5 Arnell, V.: Description and Validation of the CTH-Urban Runoff Model. 1980.

A:6 Sjöberg, A.: Calculation of Unsteady Flows in Regulated Rivers and Storm Sewer Systems. 1976.

A:7 Svensson, T.: Water Exchange and Mixing in Fjords. Mathematical Models and Field Studies in the Byfjord. 1980.

A:8 Arnell, V.: Rainfall Data for the Design of Sewer Pipe Systems. 1982.

A:9 Lindahl, J., Sjöberg, A.: Dynamic Analysis of Mooring Cables. 1983.

A:10 Nilsdal, J-A.: Optimeringsmodellen ILSD. Beräkning av topografins inverkan på ett dagvattensystems kapacitet och anläggningskostnad. 1983.

A:11 Lindahl, J.: Implicit numerisk lösning av rörelseekvationerna för en förankrings-kabel. 1984.

A:12 Lindahl, J.: Modellförsök med en förankringskabel. 1985.

A:13 Lyngfelt, S.: On Urban Runoff Modelling. The Application of Numerical Models Based on the Kinematic Wave Theory. 1985.

A:14 Johansson, M.: Transient Motions of Large Floating Structures. 1986.

A:15 Mårtensson, N., Bergdahl, L.: On the Wave Climate of the Southern Baltic. 1987.

A:16 Moberg, G.: Wave Forces on a Vertical Slender Cylinder. 1988.

A:17 Perrusquía González, G.S.: Part-Full Flow in Pipes with a Sediment Bed. Part one: Bedform dimensions. Part two: Flow resistance. 1988.

A:18 Nilsdal, J-A.: Bedömning av översvämningsrisken i dagvattensystem. Kontrollberäkning med typregn. 1988.

A:19 Johansson, M.: Barrier-Type Breakwaters. Transmission, Reflection and Forces. 1989.

A:20 Rankka, W.: Estimating the Time to Fatigue Failure of Mooring Cables. 1989.

A:21 Olsson, G.: Hybridelementmetoden, en metod för beräkning av ett flytande föremåls rörelse. 1990.

A:22 Perrusquía González, G.S.: Bedload Transport in Storm Sewers. Stream Traction in Pipe Channels. 1991.

A:23 Berggren, L.: Energy Take-Out from a Wave Energy Device. A Theoretical Study of the Hydrodynamics of a Two Body Problem Consisting of a Buoy and Submerged Plate. 1992.

CHALMERS TEKNISKA HÖGSKOLA
Institutionen för vattenbyggnad

Report Series B

B:1 Bergdahl, L.: Beräkning av vågkrafter. (Ersatts med 1979:07) 1977.

B:2 Arnell, V.: Studier av amerikansk dagvattenteknik. 1977.

B:3 Sellgren, A.: Hydraulic Hoisting of Crushed Ores. A feasibility study and pilot--plant investigation on coarse iron ore transportation by centrifugal pumps. 1977.

B:4 Ringesten, B.: Energi ur havsströmmar. 1977.

B:5 Sjöberg, A., Asp, T.: Brukar-anvisning för ROUTE-S. En matematisk modell för beräkning av icke-stationära flöden i floder och kanaler vid strömmande tillstånd. 1977.

B:6 Annual Report 1976/77. 1977.

B:7 Bergdahl, L., Wernersson, L.: Calculated and Expected Thermal Ice Pressures in Five Swedish Lakes. 1977.

B:8 Göransson, C-G., Svensson, T.: Drogue Tracking - Measuring Principles and Data Handling. 1977.

B:9 Göransson, C-G.: Mathematical Model of Sewage Discharge into confined, stratified Basins - Especially Fjords. 1977.

B:10 Arnell, V., Lyngfelt, S.: Beräkning av dagvattenavrinning från urbana områden. 1978.

B:11 Arnell, V.: Analysis of Rainfall Data for Use in Design of Storm Sewer Systems. 1978.

B:12 Sjöberg, A.: On Models to be used in Sweden for Detailed Design and Analysis of Storm Drainage Systems. 1978.

B:13 Lyngfelt, S.: An Analysis of Parameters in a Kinematic Wave Model of Overland Flow in Urban Areas. 1978.

B:14 Sjöberg, A., Lundgren, J., Asp, T., Melin, H.: Manual för ILLUDAS (Version S2). Ett datorprogram för dimensionering och analys av dagvattensystem. 1979.

B:15 Annual Report 1978/79. 1979.

B:16 Nilsdal, J-A., Sjöberg, A.: Dimensionerande regn vid höga vattenstånd i Göta älv. 1979.

B:17 Stöllman, L-E.: Närkes Svartå. Hydrologisk inventering. 1979.

B:18 Svensson, T.: Tracer Measurements of Mixing in the Deep Water of a Small, Stratified Sill Fjord. 1979.

B:19 Svensson, T., Degerman, E., Jansson, B.,Westerlund, S.: Energiutvinning ur sjö- och havssediment. En förstudie. R76:1980. 1979.

B:20 Annual Report 1979. 1980.

B:21 Stöllman, L-E.: Närkes Svartå. Inventering av vattentillgång och vattenanvändning. 1980.

Report Series B

B:22 Häggström, S., Sjöberg, A.: Effects of Distortion in Physical Models of Cooling Water Discharge. 1979.

B:23 Sellgren, A.: A Model for Calculating the Pumping Cost of Industrial Slurries. 1981.

B:24 Lindahl, J.: Rörelseekvationen för en kabel. 1981.

B:25 Bergdahl, L., Olsson, G.: Konstruktioner i havet. Vågkrafter-rörelser. En inventering av datorprogram. 1981.

B:26 Annual Report 1980. 1981.

B:27 Nilsdal, J-A.: Teknisk-ekonomisk dimensionering av avloppsledningar. En litteraturstudie om datormodeller. 1981.

B:28 Sjöberg, A.: The Sewer Network Models DAGVL-A and DAGVL-DIFF. 1981.

B:29 Moberg, G.: Anläggningar för oljeutvinning till havs. Konstruktionstyper, dimensioneringskriterier och positioneringssystem. 1981.

B:30 Sjöberg, A., Bergdahl, L.: Förankringar och förankringskrafter. 1981.

B:31 Häggström, S., Melin, H.: Användning av simuleringsmodellen MITSIM vid vattenresursplanering för Svartån. 1982.

B:32 Bydén, S., Nielsen, B.: Närkes Svartå. Vattenöversikt för Laxå kommun. 1982.

B:33 Sjöberg, A.: On the stability of gradually varied flow in sewers. 1982.

B:34 Bydén, S., Nyberg, E.: Närkes Svartå. Undersökning av grundvattenkvalitet i Laxå kommun. 1982.

B:35 Sjöberg, A., Mårtensson, N.: Regnenveloppmetoden. En analys av metodens tillämplighet för dimensionering av ett 2-års perkolationsmagasin. 1982.

B:36 Svensson, T., Sörman, L-O.: Värmeupptagning med bottenförlagda kylslangar i stillastående vatten. Laboratorieförsök. 1982.

B:37 Mattsson, A.: Koltransporter och kolhantering. Lagring i terminaler och hos storförbrukare. (Delrapport). 1983.

B:38 Strandner, H.: Ett datorprogram för sammankoppling av ILLUDAS och DAGVL-DIFF. 1983.

B:39 Svensson, T., Sörman, L-O.: Värmeupptagning med bottenförlagda slangar i rinnande vatten. Laboratorieförsök. 1983.

B:40 Mattsson, A.: Koltransporter och kolhantering. Lagring i terminaler och hos storförbrukare. Kostnader. Delrapport 2. 1983.

B:41 Häggström, S., Melin, H.: Närkes Svartå. Simuleringsmodellen MITSIM för kvantitativ analys i vattenresursplanering. 1983.

B:42 Hård, S.: Seminarium om miljöeffekter vid naturvärmesystem. Dokumentation sammanställd av S. Hård, VIAK AB. BFR-R60:1984. 1983.

B:43 Lindahl, J.: Manual för MODEX-MODIM. Ett datorprogram för simulering av dynamiska förlopp i förankringskablar. 1983.

Report Series B

B:44 Activity Report. 1984.

B:45 Sjöberg, A.: DAGVL-DIFF. Beräkning av icke-stationära flödesförlopp i helt eller delvis fyllda avloppssystem, tunnlar och kanaler. 1984.

B:46 Bergdahl, L., Melin, H.: WAVE FIELD. Manual till ett program för beräkning av ytvattenvågor. 1985.

B:47 Lyngfelt, S.: Manual för dagvattenmodellen CURE. 1985.

B:48 Perrusquía, G., Lyngfelt, S., Sjöberg, A.: Flödeskapacitet hos avloppsledningar delvis fyllda med sediment. En inledande experimentell och teoretisk studie. 1986.

B:49 Lindahl, J., Bergdahl, L.: MODEX-MODIM. User's Manual. 1987.

B:50 Mårtensson, N.: Dynamic Analysis of a Moored Wave Energy Buoy. 1988.

B:51 Lyngfelt, S.: Styrning av flöden i avloppssystem. Begrepp - Funktion - FoU-Behov. 1989.

B:52 Perrusquía, G.: Sediment in Sewers. Research Leaves in England. 1990.

B:53 Lyngfelt, S.: Simulering av ytavrinning i dagvattensystem. 1991.

B:54 Lyngfelt, S.: Two papers on Urban Runoff Modelling:
Base Catchment Modelling in Urban Runoff Simulation and An Improved Rational Method for Urban Runoff Application. 1991.